Attachment 1 to the Seismic Hazards Report for the Exelon Generation Company, LLC Early Site Permit

Site Safety Analysis Report Appendix B

Contents

1. Paleoliquefaction Investigations B1-1-1
1.1 Previous Investigations in Southern Illinois Basin Region B1-1-2
1.2 Completeness of Paleoliquefaction Record B1-1-5
1.3 Estimating Source Areas and Magnitudes of Paleoearthquakes B1-1-5
1.4 Paleoliquefaction Investigations in the Site Vicinity B1-1-6
1.4.1 Criteria for Identifying Clastic Dikes of Seismic Origin B1-1-8
1.4.2 Possible Paleoliquefaction Features B1-1-9
1.4.2.1 Locality SC 25 ..... B1-1-9
1.4.2.2 Locality SC 16 ..... B1-1-11
1.4.2.3 Locality SC 19/SC 18 ..... B1-1-12
1.4.2.4 Locality M 6 ..... B1-1-13
1.4.3 Evidence for the Absence of Paleoliquefaction B1-1-15
1.4.4 Conclusions B1-1-16
2. References B1-2-1

Tables

B-1-1 Liquefaction Evidence for Prehistoric Earthquakes in the Southern Illinois Basin B1.T-1
B-1-2 Summary of Deposits in Bank Exposures B1.T-6
B-1-3 Criteria for Differentiating Origins of Liquefaction Features B1.T-7
B-1-4 Characteristics and Estimated Ages of Potential Liquefaction Features Identified in Site Vicinity B1.T-9
B-1-5 Localities of Older Alluvium B1.T-10

Figures

B-1-1 Epicenters of Historical Earthquakes and Estimated Energy Centers of Large Prehistoric Earthquakes in Site Region
B-1-2 Sites of Paleoliquefaction in Southern Indiana and Illinois
B-1-3 Map of Vicinity of the Springfield, Illinois, Earthquake Showing Approximate Limit of Liquefaction
B-1-4A Moment Magnitude versus Maximum Distance to Surface Evidence of Liquefaction
B-1-4B Revised Region-specific Magnitude Bound Relation for Central United States
B-1-5 Map Showing Bedrock Structures, Geophysical Lineaments, and Paleoearthquake Energy Centers
B-1-6 Map Showing Surveyed Stream Banks and Evidence for Paleoliquefaction in the Site Vicinity
B-1-7 Areal Distribution of the Wedron and Mason Groups (Wisconsin and Hudson Episodes) and Deposits of the Illinois and Pre-Illinois Episodes in Illinois
B-1-8 Areal Distribution of Moraines and Boundaries of Formations and Principal Members of the Wedron Group
B-1-9 Geochronologic Units, Chronostratigraphic Units, and Diachronic Units in the Lake Michigan Lobe
B-1-10 Photograph of Riverbank Exposure on Salt Creek Showing Fluvial Terrace Deposits of Two Ages
B-1-11 Map of Quaternary Deposits in Site Vicinity
B-1-12 Flow Chart Showing Seismic and Nonseismic Mechanisms That Create Deformation Features in Sediment
B-1-13A Photographs of Dike 1 at Locality SC 25
B-1-13B Photographs of Dike 1 at Locality SC 25
B-1-14 Photograph of Dike 2 at Locality SC 19
B-1-15A Photographs of Parts of Dike 1 at Locality M 6
B-1-15B Photographs of Parts of Dike 1 at Locality M 6
B-1-16 Photograph of Thick Silt Layer Overlaying Fluvial Deposit at Locality S 14

Exhibit

1 Radiocarbon Dating

CHAPTER 1

Paleoliquefaction Investigations

In the central and eastern United States (CEUS), seismogenic faults are uncommon or difficult to identify. Strain rates are relatively low, and recurrence intervals for large earthquakes are usually longer than the historical record. In this tectonic environment, identification of liquefaction or other features resulting from strong ground motion has proven to be an effective tool in identifying and characterizing seismogenic sources that generated moderate- to large-magnitude earthquakes in prehistoric time.

Earthquake-induced liquefaction is understood to be a process by which saturated, granular sediment temporarily loses its strength in response to earthquake ground shaking. Relatively cohesionless sediment that is water-saturated and loosely packed will tend to compact, leading to an increase in pore water pressure. If pore water pressure increases to the point that it equals overburden pressure, the sediment can behave as a viscous liquid. Under certain conditions the resulting slurry of sediment and water will tend to flow toward the ground surface, forming a number of distinctive sedimentary features, including sand blows (or boils), dikes, and sills.

Recent papers by Obermeier (1996), Obermeier et al. (2001 and 2002), Tuttle (2001), Olson et al. (2003, revised January 2004), and Green et al. (2004a, 2004b), review the criteria and multi-step process by which features of seismically induced liquefaction are identified and used to evaluate the timing, location of source area, and magnitude of the causative earthquake. These papers summarize and critique issues concerning field methods for identifying paleoliquefaction features, as well as the interpretation and back-analysis of strength of shaking and earthquake magnitude using geologic and geotechnical/seismologic procedures.

Recent studies in the region of the Exelon Generation Company (EGC) site that is the subject of this Early Site Permit (ESP) application have identified energy centers for several prehistoric moderate- to large-magnitude earthquakes in southern and central Illinois based on evidence of paleoliquefaction. Those studies show the usefulness of paleoliquefaction investigations in demonstrating a longer seismic record than provided by historical seismicity alone. The results of those studies were used to evaluate the earlier expert assessment of seismic sources in the CEUS performed by the Electric Power Research Institute (EPRI) Seismicity Owners' Group (SOG). In particular, the results of recently published studies suggest that the range of maximum magnitude for the regional background sources defined by the EPRI-SOG teams may be insufficient. Paleoliquefaction studies previously had not been conducted throughout most of the region within a 25-mile radius of the EGC ESP Site. A reconnaissance field study was conducted as part of the current ESP application to supplement previously published studies and to provide more site-specific information that could be used to better evaluate the estimated magnitude of a background earthquake. The results of previous and current field studies are summarized below.

1.1 Previous Investigations in Southern Illinois Basin Region

The Illinois basin encompasses most of Illinois and nearby parts of southwest Indiana and western Kentucky. The southern Illinois basin region is characterized by persistent, scattered seismicity that includes several moderate-magnitude historical earthquakes. The field investigation of liquefaction features at several sites indicates that multiple paleoearthquakes having magnitudes significantly larger than historical events have occurred in the region (Figure B-1-1).

Mapping and dating of liquefaction features throughout most of the southern Illinois basin (in parts of Indiana, Illinois, and Missouri) have identified epicentral areas for at least eight Holocene and latest Pleistocene earthquakes of estimated moment magnitude **M** 6 to ~ 7.8 (Figures B-1-1 and B-1-2) (Obermeier et al., 1991; Munson et al., 1997; Pond and Martin, 1997; Tuttle et al., 1999; Obermeier, 1998; McNulty and Obermeier, 1999). The energy sources (and inferred epicenters) for the identified paleoliquefaction evidence occur within Indiana and Illinois, except for the youngest features, observed in Cache Valley in southernmost Illinois, that probably were induced by the great New Madrid, Missouri, earthquakes of 1811-1812 (Obermeier, 1998). Evidence for the location, size, and timing of those prehistoric events is summarized in Table B-1-1. Discussed below are the identified events that are closest and most significant to the assessment of seismic hazard at the EGC ESP Site.

Lower Wabash Valley Earthquakes — The magnitude of the largest paleoearthquake in lower Wabash Valley (the Vincennes-Bridgeport earthquake), which occurred 6,100 ± 200 yr. BP[1], was estimated to be ≥ **M** 7.5 using the magnitude-bound method (Obermeier, 1998). Use of a more recently developed magnitude-bound curve for the CEUS based on a value of **M** ~7.6-7.7 for the largest of the 1811-1812 New Madrid earthquakes (reduced from the higher **M** 8 used in the older curve) and review of other historical events gives a lower estimate of **M** 7.3 (Olson et al., 2005, in press). A re-analysis of this earthquake by Green et al. (2004a, 2004b) using more recent ground motion attenuation relationships for the central United States; review of boring logs presented by Pond to select appropriate SPT values for the re-analysis; and 2001 NEHRP site amplification factors gives lower results. Based on this analysis, Green et al. (2004a, 2004b) estimate the magnitude of the Vincennes earthquake was approximately **M** 7.5. The more recent evaluations by Green et al. have considered the influence of aging effects on liquefaction susceptibility and concluded that for moderately susceptible sites such as those in southern Illinois, the small changes expected given the types of sediments would have little influence on the interpretation of paleomagnitude (Obermeier et al., 2001, 2002; Green et al., 2004a, 2004b).

Skelton-Mt. Carmel Earthquake – The next-largest earthquake (the Skelton-Mt. Carmel earthquake) occurred 12,000 ± 1,000 yr. BP (Hajic and Wiant, 1997; Munson et al., 1997; Obermeier, 1998). This earthquake is estimated to have been **M** 7.1 to 7.2 by Munson et al. (1997) and **M** 7.3 by Pond and Martin (1997). Based on a revised magnitude-bound relation (Olson et al., 2005, in press), give a best estimate of **M** 6.7. Both this and the Vincennes-Bridgeport earthquake were close to one another and took place in the general vicinity of the most numerous and strongest historical earthquakes (**M** 4 to 5.5) in the lower Wabash

[1] Ages reported are uncorrected radiocarbon years BP (before present), except where noted (i.e., for calendar ages reported as BC or AD).

Valley of Indiana-Illinois (Obermeier, 1998). The inferred locations of the energy sources for these events are approximately 15 miles west and 25 miles southwest of Vincennes, Indiana, respectively (Figures B-1-1 and B-1-2).

Springfield and Shoal Creek Earthquakes – Paleoearthquakes of lower magnitude, as indicated by paleoliquefaction features, are more randomly distributed, commonly having struck in regions having no significant historical seismicity. Smaller paleoearthquakes recorded by liquefaction features in Indiana, described in Table B-1-1, include at least three events that occurred east of the lower Wabash Valley source region in central and southern Illinois. In this area two strong, mid-Holocene earthquakes, referred to as the Springfield and Shoal Creek earthquakes, are documented by paleoliquefaction features such as clastic dikes, sills, and detachments of fine-grained sediment that sank into liquefied sand (McNulty and Obermeier, 1999).

Springfield Earthquake—Evidence for a prehistoric earthquake near Springfield, Illinois, was first discovered by Hajic in 1994 (Hajic et al., 1995). Subsequent field investigations documented at least one moderate-sized earthquake (**M** 6.2 to 6.8) and probably a second smaller event (minimum magnitude of ~ **M** 5.5) in the region between 5,900 and 7,400 yr. BP (McNulty and Obermeier, 1999). Based on the areal extent of paleoliquefaction and the location of the largest dike observed (15 inches [37 cm] wide), the source of the larger event was centered about 22 miles northeast of Springfield, Illinois (Figure B-1-3). Both events may have had approximately the same source location and extent of liquefaction, but data are insufficient to confirm this conclusion.

The McNulty and Obermeier (1999) estimate of the magnitude of the Springfield earthquake was based on the maximum distance of paleoliquefaction features from the inferred energy center (approximately 22 miles [35 km]) compared to curves that relate moment magnitude versus maximum distance to surface evidence of liquefaction (Figure B-1-4A). McNulty and Obermeier (1999) state that **M** 6.8 represents an upper-bound estimate for this earthquake, citing evidence for a high water table at the time of the earthquake and relatively shallow depth to bedrock that would limit amplification of bedrock shaking. Based on a revised magnitude-bound relation presented in Olson et al. (2005, in press), the estimated magnitude of this earthquake is **M** 6.3 (Figure B-1-4B).

There are no readily apparent geologic structures that can serve as strong candidates for the causative source for the Springfield earthquake(s). Only two small structures are mapped within the recognized source region of the Springfield event(s) as defined by the observed paleoliquefaction features. These structures are a small (< 6 miles-long), generally northwest-trending domal structure and a 10-mile-long north-northwest-trending fold and associated fault (Figure B-1-5). The apparent localization of liquefaction features may relate more to thickness and susceptibility of local sediment, so that the energy source for an event may not be coincident with the larger liquefaction features, but rather with a more distant, larger earthquake (R. Bauer, Illinois Geological Survey, personal communication, November 21, 2002).

Shoal Creek Earthquake—Paleoliquefaction evidence shows that a strong earthquake occurred in southwest Illinois at about 4,520 BC ± 160 yr., or 6,500 years ago (also 5,670 ± 80 radiocarbon years BP) (McNulty and Obermeier, 1999; Tuttle et al., 1999). McNulty and Obermeier (1999) infer the energy source to be about 50 miles east-southeast of St. Louis,

Missouri, in the vicinity of lower Shoal Creek where there are dikes as wide as 1.6 feet (0.5 m), and there is a concentration of dike sites (Figure B-1-2). Dikes from this event as mapped by McNulty and Obermeier extend approximately 22 miles (35 km) from the inferred energy source. Tuttle et al. (1999) report prehistoric Holocene dikes at sites immediately south and east of St. Louis (see discussion below). They suggest that the energy source for all liquefaction sites near St. Louis and Shoal Creek was east of St. Louis, likely at the location inferred by McNulty and Obermeier (1999). However, they also suggest plausible sources nearer to St. Louis, or on the Centralia fault east of the Shoal Creek center shown on Figure B-1-2. McNulty and Obermeier (1999) believe that the source may be nearer to St. Louis, but based on the absence of dikes immediately east of the Kaskaskia River, they discount a source centered there.

Evidence for at least two earthquakes, widely spaced in time, is represented by the dikes within the approximate limit of liquefaction in the Shoal Creek area, as shown on Figure B-1-2. Although multiple events are indicated in the Shoal Creek region, the level of ground motion appears to have been significantly different during the two events, suggesting that the younger event was either of significantly lower magnitude or from a more distant source. The younger dikes are rare and small within deposits younger than mid-Holocene, indicating the absence of very strong ground shaking since that time. These features may have been caused by the 1811-1812 great New Madrid earthquakes (McNulty and Obermeier, 1999).

The magnitude of the Shoal Creek earthquake probably exceeded **M** 6. Based on comparison to the magnitude versus maximum distance of paleoliquefaction curves, a reasonable lower limit seems to be about **M** 6.5 (McNulty and Obermeier, 1999). The revised magnitude-bound relation (Olson et al., 2005, in press), gives a lower estimate of **M** 6.3.

The closest major mapped bedrock structure to the energy source for the Shoal Creek earthquake is the Centralia fault, which is associated with the Du Quoin monocline approximately 12 miles to the east (Figure B-1-5). The distribution of paleoliquefaction features associated with this event suggests an energy source west of the Centralia fault. Other small folds (< 6 miles long) are mapped at similar distances northeast, south, and southwest of the inferred energy center.

Southeastern Missouri (St. Louis area) -- A sand sill, associated dikes, and other liquefaction features along the Big Muddy River formed since 9,070 BC and possibly prior to 4,240 BC (Tuttle et al., 1999). In addition, sand dikes along the Meramec River near St. Louis appear to be prehistoric and to have formed since 13,210 BP. It is possible, but not necessary, that these features formed as a result of the same earthquake responsible for the middle-Holocene liquefaction features in the Shoal Creek region. Tuttle et al. (1999) consider three alternative scenarios for the formation of these features: a **M** 7.5 earthquake on the Centralia fault; a **M** 7.0 centered near Germantown, Illinois, near the largest features on Shoal Creek; or a **M** > 5.2 near St. Louis.

Based on the spatial distribution of prehistoric liquefaction features, mapped faults, and modern seismicity in the region northwest of the New Madrid seismic zone, Tuttle et al. (1999) suggest that possible paleoearthquake sources include the Valmeyer and Waterloo-Dupo anticlines; Du Quoin monocline; Centralia, St. Louis, and New Madrid faults; and an unidentified source near Shoal Creek and Germantown, Illinois. They conclude, however,

that poor age constraints make it difficult to draw regional correlations of liquefaction features and to estimate magnitudes of causative earthquakes, and that any of the alternative scenarios described above could explain the distribution of paleoliquefaction in southern Illinois and southeast Missouri.

1.2 Completeness of Paleoliquefaction Record

Previous workers have noted that additional moderate- to large-magnitude earthquakes may have occurred within the southern Illinois basin that cannot be detected with present methods. Obermeier (1998) discusses several factors to be considered, such as the few known liquefaction features that cannot be assigned to one of the eight postulated prehistoric earthquakes, the few known liquefaction features older than 12 ka[2], the areas that have not been studied, and the lack of liquefiable deposits or local sedimentalogic and hydrologic conditions that affect the magnitude threshold for liquefaction. He concludes that the record is most likely to be complete for earthquakes that are most recent, particularly larger earthquakes. He suggests that probably no prehistoric earthquake larger than **M** 7 has been overlooked in southern Illinois or southwestern Indiana, but that ten or more Holocene or latest Pleistocene earthquakes of **M** 6 to 7 might have been overlooked because of lack of nearby liquefiable deposits.

1.3 Estimating Source Areas and Magnitudes of Paleoearthquakes

As discussed above, the size distribution of liquefaction features commonly is assumed to reflect the source region of a paleoearthquake. Tuttle et al. (1999) note that empirical data from historical earthquakes (e.g., 1988 Saguenay, Quebec; 1989 Loma Prieta; and 1994 Northridge) show that the distribution of liquefaction features can be irregular and not necessarily centered around or even within the meizoseismal area. Factors that influence the distribution of liquefaction features include earthquake characteristics, such as directivity and focusing of seismic waves, and site conditions, such as liquefaction susceptibility of sediments, local ground motion amplification, and topography. Wheeler and Cramer (2002) note that for hazard calculations, inferring energy centers based on the size and distribution of paleoliquefaction features appears to involve uncertainties of a few tens of kilometers. They consider factors such as the non-uniform distribution of liquefiable deposits, the length of ruptures, particularly for larger events that likely would not result from a point source, directivity effects, and data from prehistoric events in Illinois and Indiana that show that the widest dikes for individual events are found 6 to 15 miles (10 to 25 km) from the approximate centers of the corresponding liquefaction fields.

1.4 Paleoliquefaction Investigations in the Site Vicinity

Both field reconnaissance and detailed field investigations in the vicinity of the EGC ESP Site have been conducted along sections of several larger streams, including the Sangamon

[2] ka (thousands of years before present)

River, South Fork of the Sangamon River, and Salt Creek, as well as such smaller streams as Sugar Creek, Kickapoo Creek, Deer Creek, and Lake Fork (McNulty and Obermeier, 1999) (Figures B-1-2 and B-1-3). These studies provide reasonably good coverage of the region south and west, and to a lesser degree east, of the site. Geomatrix performed reconnaissance-level investigations of rivers and streams north and east of the site to provide more complete coverage of the site region (within a radius of approximately 25 to 35 miles) (Figure B-1-6). Approximately 41 miles of river, including parts of the Mackinaw River, the Sangamon River, and the North and South forks of Salt Creek, were investigated for this study. This fieldwork was performed during a two-week period from September 23 to October 4, 2002. Dr. Stephen Obermeier, a recognized specialist in identifying and characterizing paleoliquefaction features in the central and eastern United States, participated in the field investigations and the interpretation of results.

Formation of seismically induced liquefaction features such as dikes is optimized by the following conditions: (1) liquefiable sediment (preferably a clean sand that has a thickness of 3 feet or greater); (2) an overlying thin, low-permeability soil cap—generally a cap of silt and clay at least 3 and less than 30 feet thick (optimally about 6 to 16 feet); and (3) a shallow water table (optimally less than 16 feet deep). Liquefaction-induced features can form even where the top of the overlying cap is submerged by many feet of water. Obermeier et al. (2001 and 2002) discuss the basic mechanisms that induce seismic liquefaction features. Dikes in a fine-grained cap form chiefly by three ground failure mechanisms: hydraulic fracturing, lateral spreading, and surface oscillations. These three mechanisms can occur independently or in combination.

The drainages in the study area are incised into till plains and moraine systems associated with the late Wisconsin-age Lake Michigan lobe (Hansel and Johnson, 1996) (Figures B-1-7 through B-1-9). Deposits of the Wisconsin Episode of glaciation in Illinois record migrating proglacial and glacial environments that are classified into two intertonguing groups. The diamictons, including till and ice-marginal deposits, are classified in the Wedron Group. The sorted proglacial sediment deposits, primarily loess, eolian sand, lake sediment, and outwash, are classified in the Mason Group (Figures B-1-7 and B-1-9). The larger streams cut through broad valleys where the highest terraces are composed of Wisconsinan glaciofluvial and early Holocene braid-bar deposits of thick, clean sand. The sands are capped by fine-grained overbank and loess material that can reach 10 to 15 feet in thickness. These highest terraces are generally about 15 feet above the low flow level of the modern streams. Inset into these terraces are younger deposits that include point-bar sediments (primarily sandy gravel, gravelly sand, and sand) from streams having a meandering character (Figures B-1-10 and B-1-11). The sand and gravel deposits, both of braid bars in low terraces and of point bars, usually are capped abruptly by 6 to 15 feet of fine-grained (sandy silt to clayey silt) alluvium, primarily from overbank and channel-fill deposits. The degree of soil development in the fine-grained cap generally reflects the age of the sediments.

In the study area, deposits older than mid-Holocene (> 6 to 7 ka) are recognized by weathering profiles that exhibit oxidation in fine-grained sediments to depths at and below the modern depth of the water table. Obermeier (1998) notes that these weathering profiles were imposed chiefly during the early to middle Holocene, when the climate was generally

warmer and drier than at present. This period of warm, dry weather commonly is referred to as the "hypsithermic."

The following general approach was used in this study to identify sites having conditions favorable for the development and preservation of paleoliquefaction features.

1. The Quaternary geologic map for the State of Illinois (Lineback, 1979) was used to identify reaches of the larger streams within the study region (~ 40- to 56-mile radius of the site) where deposits of the late Wisconsin Henry Formation have been mapped (Figure B-1-11). The Henry Formation includes generally well-sorted sand and gravel deposited as glacial outwash in outwash plains, as valley train, or as ice-contact sediments. In areas of high groundwater, these sediments would be susceptible to liquefaction. Where the sediments are preserved at or within a few feet (meters) of present low water along current drainages, they provide the most complete geologic record of the presence or absence of late glacial and post-glacial liquefaction.

2. A secondary tool for identifying locations where deposits of latest Pleistocene to early Holocene age may be preserved along present drainages were the U.S. Department of Agriculture Soil Conservation Survey (Soil Survey) maps for DeWitt, McClean, and Champaign counties. These maps were used to identify more specific locations where well-developed soils might be found in appropriate parent material (loess, glaciofluvial outwash terraces, or early Holocene alluvium).

3. U.S. Geological Survey 7.5-minute quadrangle topographic maps also were reviewed to identify geomorphic surfaces of latest Pleistocene to early Holocene age and to identify gravel pit operations that would provide accessible subsurface exposures.

The Geomatrix field reconnaissance was performed by examining banks of streams and exposures in local sand and gravel pits. Recent paleoliquefaction investigations demonstrate that search of eroded banks of steams, generally from a canoe, is the best means of documenting the presence or absence of paleoliquefaction features. Optimal conditions for finding liquefaction features depend on the size of the stream. For larger streams and rivers (e.g., the Mackinaw River and the lower reaches of the Sangamon River and Salt Creek), the low-water conditions of late fall/early winter after vegetation starts to die generally offer the most continuous exposures. For smaller streams that typically are overgrown with brush and vegetation (e.g., the upper reaches and North Fork of Salt Creek), ideal conditions occur soon after flooding (early spring), when undercutting of the stream creates new bank exposures. The larger streams examined during this study had relatively low water levels, which provided good exposures at and slightly above stream level. The low water, however, limited access by canoe to the upper reaches of the drainages. Continuous reconnaissance along limited stretches of these reaches was conducted by walking. These relatively continuous reconnaissance-level investigations were supplemented by additional reconnaissance at targeted stream and gravel pit locations easily accessible from roads or bridge crossings.

In an average day, 3 to 5 miles of river bank could be searched. Access by canoe was limited along some heavily wooded sections where log jams were common. The degree of exposure of susceptible deposits varied along the stretches of the rivers studied (Table B-1-2). Typically, approximately 5 to 7 percent of the banks revealed "pre-hypsithermic" deposits of mid-Holocene (at least 5,000 years old) to earlier Holocene age (~ 6 to 10 ka). Exposures of older latest Pleistocene alluvium were much more limited. Many bank exposures, particularly the youngest (late Holocene terrace deposits), were masked by a thin veneer of colluvium or slope wash and vegetation. However, the relatively low water levels in larger streams generally provided sufficient exposure of the lowermost 1 to 2 feet, particularly for older (pre-hypsithermic) deposits. The degree of exposure along larger streams and rivers in the study area was comparable to that observed in the Springfield study region. Along smaller streams, however, exposures in the Springfield area, which were investigated shortly after record floods, were more frequent and complete than those observed during this study. Overall, the reconnaissance performed for the EGC ESP project provided a reasonable opportunity to find clastic dikes that had formed throughout the Holocene, and especially since the mid-Holocene (post-hypsithermic) throughout the study area.

The objective of the field reconnaissance was to document the presence or absence of paleoliquefaction features in the vicinity of the EGC ESP Site. Liquefaction features of latest Pleistocene/early Holocene and mid-Holocene age were identified at isolated localities in the study area. The following sections present the criteria for differentiating seismic from nontectonic origins of liquefaction features, followed by descriptions of the features observed and interpretations of the likely origin or triggering event for each feature.

1.4.1 Criteria for Identifying Clastic Dikes of Seismic Origin

The clastic dikes and possible sills identified during this investigation exhibit many characteristics in common with seismically induced paleoliquefaction features. However, nonseismic mechanisms may produce clastic dikes or other deformational features in sediments that may be difficult to distinguish from those that represent seismically induced liquefaction. As noted by others (e.g., Tuttle, 2001; Obermeier, 1996 and 1998), nonseismic mechanisms that should be considered include dewatering due to rapid sedimentation and compaction, artesian pressure, and, during floods, piping and diversion of runoff that may produce sand boils (Figure B-1-12).

In addition, in glaciated regions, clastic dikes comprising fluid escape structures, glaciogenic injections, and fluidal and viscous hydraulic expulsions may form in response to subglacial melting and dewatering (Broster, 1991; Dreimanis and Rappol, 1997). Alternative mechanisms postulated to explain formation of these features include Broster's (1991) model involving expulsion of pore water from confined layers and consolidation and fracturing of subglacial sediments by overriding grounded ice. He notes that most deformation structures formed by expulsion reflect initial overriding and compaction of saturated sediments, with this compaction producing hydraulic conditions that favor release of pore water. Correlation with directions of glacial movement, association with glacial facies (e.g., termination at the base of overlying till), and infilling by glacial sediments are considered to be glaciogenic signatures useful in differentiating glacial from nonglacial (e.g., earthquake) origins for similar features (Broster, 1991).

As synthesized by Obermeier (1996) and summarized below, criteria for identifying earthquake-induced liquefaction features include:

1. sedimentary characteristics indicative of sudden, strong, upwardly directed hydraulic force of short duration;
2. sedimentary characteristics consistent with case histories of earthquake-induced liquefaction (e.g., the meizoseismal zone of the 1811-1812 New Madrid earthquakes);
3. occurrence of similar features at multiple locations;
4. occurrence in geomorphic settings where the hydraulic conditions described in No. 1 above would not develop under nonseismic conditions; and
5. age data to support both contemporaneous and episodic formation of the features over a large area.

Specific criteria (sedimentary and stratigraphic characteristics of host deposits and material source, conduit morphology, distribution pattern, etc.) that may be used to assess the origin of possible liquefaction features identified in this study are listed in Table B-1-3. These features are described below.

1.4.2 Possible Paleoliquefaction Features

Possible liquefaction features were observed at four localities in the study area, three along Salt Creek (Localities SC 25, SC 16, and SC 19/SC 18), and one along the Mackinaw River (Locality M 6) (Figure B-1-6). The characteristics of these features and the stratigraphic relationships and ages of the associated deposits are described in general below. Table B-1-4 summarizes the estimated age and preferred interpretation for each feature.

1.4.2.1 Locality SC 25

Locality SC 25 lies approximately 5-½ miles northeast of Farmer City, Illinois, on Salt Creek. At Locality SC 25, there is an approximately 11 feet-high terrace exposure that extends approximately 300 feet along the left stream bank, providing varying degrees of exposure. The exposure generally consists of an ~ 8-foot-thick silty loess cap overlying medium to coarse sand and gravel of probable glaciofluvial origin. Within this 300-foot reach, the contact between the sand and overlying silt was exposed intermittently for a cumulative 100 feet, and the upper 6 feet of the silt cap was exposed for a cumulative 180 feet. The Soil Survey of McLean County maps this area as Tama silt loam, a moderately well-drained soil that typically forms on uplands, loess plains, terraces, and outwash plains. They describe a typical Tama silt loam as a very dark gray, friable silt loam from a depth of 0 to 12 inches; underlain by brown friable silty clay loam to a depth of 16 inches; underlain by dark yellowish brown, friable, silty clay loam that is mottled in the lower part extending to 46 inches; followed by a dark yellowish brown, mottled, friable silt loam that extends to 60 inches and beyond. Field observations noted that the soil at Locality SC 25 is similar to that described as a typical Tama silt loam.

The most recent glacial flooding on the main fork of Salt Creek likely deposited the gravel and sand exposed at the base of this sequence. Leon Follmer of the Illinois State Geological

Survey (Personal Communication, October 15, 2002) estimates this event occurred around 17 ka, when the Bloomington moraine (labeled "B" on Figure B-1-8) was breached near the town of Saybrook, Illinois (Figure B-1-11). Follmer suggests that during this event most of the floodwater drained down the Sangamon River, but overflow likely would have flowed down Salt Creek. The age of 17 ka is consistent with numerical ages and relative ages of various members of the Tiskilwa and Lemont formations from Hansel and Johnson (1996). The loess that constitutes most of the upper 8 feet of exposure at Locality SC 25 likely was deposited soon (within several hundred years) after the final flood event. Based on the above information and the relatively deeply developed soil, the deposits in exposure at Locality SC 25 is estimated to be approximately 16 to 17 ka.

The silt cap at Locality SC 25 is intruded by 6 sand dikes (Dikes 1 through 6). These dikes range in width from ~ ¼ inch to 4 inches, and in height above the sand-silt contact from ~1 foot to more than 6 feet. The dikes are described briefly below.

- Dike 1 protrudes approximately 6.3 feet up from the gravelly sand (Figures B-1-13A&B) into the silt cap, approaching within 20 inches of the ground surface, where it measures ~ 2 inches wide. This complex dike strikes nearly parallel to the exposure, but also bifurcates, with some branches oriented nearly perpendicular to the wall. It also includes apparently disjointed segments at its lower end (Figure B-1-13B). Dike 1 can be traced for ~ 13 feet along the stream bank. The dike fill material ranges from clean, oxidized, medium-grained sand near the top, to oxidized gravelly sand near the base.

- Dike 2 occurs high on the stream bank, extending to within 3 feet of the modern ground surface. It consists of two narrow (approximately 0.5-inch-wide), tabular, subvertical dikes that extend 2 feet above and 6 inches below a horizontal sill that measures 6 inches long by 2 inches thick. The entire feature is filled with oxidized, uniform, fine-grained sand. Dike 2 is exposed well above the sand-silt contact, and therefore is not associated directly with the gravelly sand at the base of the exposure.

- Dikes 3, 4, and 5 each consists of thin (0.25- to 0.5-inch-thick), tabular dikes that extend a short distance (1 to 1.5 feet) up from the gravelly sand into the overlying silt. Each has sharp contacts and is filled with fine- to medium-grained, oxidized sand.

- Dike 6 intrudes the silt unit to within approximately 2.5 feet of the modern ground surface. This complex dike reaches a maximum width of 2.5 inches and is exposed clearly for more than 4 vertical feet. It consists of a prominent subvertical dike oriented at an ~ 60-degree angle to the exposure wall and two narrower (approximately 1-inch-wide) dikes, oriented roughly parallel to the exposure wall, that join the main dike and extend out from it. These secondary dikes can be traced along the exposure wall for a distance as great as 3 feet. Additionally, a narrow (~ 0.25-inch-wide) dike intrudes the silt approximately 3 feet downstream of the main dike, striking parallel to it. Although the dikes at this locality are roughly tabular in shape, their walls are very irregular. Near the base, the dike filling consists of oxidized gravelly sand, which grades upward to fine sand near the top. The filling includes irregular, angular clasts of silt (wall

rock) that measure as much as 1 inch in diameter. This dike system could not be traced clearly into the gravelly sand below, because much of the lower part of the exposure was covered, but it does approach to within 1.5 feet of the lower unit.

The dikes observed at Locality SC 25 display many characteristics common in seismic liquefaction features (Table B-1-3). They are filled with sand; have sharp, irregular side contacts; widen with depth; occur in clear association with the underlying gravelly sand (except for Dikes 2 and 6); and are generally tabular in plan view, although Dikes 1 and 6 bifurcate in multiple directions. The high degree of weathering of the material within the dikes is interpreted as evidence that they were formed during the latest Pleistocene (between approximately 10 and 17 ka).

A seismic origin is preferred for the clastic dikes observed at this locality. The locality is not in an area where high artesian pressures are known to occur (Leon Follmer, Illinois Geological Survey, personal communication, October 4, 2002), nor in a topographic setting that could produce localized artesian conditions. The features post-date the most recent glacial advance at this location and clearly are not related to glaciotectonic processes. The features at SC 25 meet criteria 1, 2, and 4 outlined above. However, the available data do not fulfill criterion 3 (the occurrence of similar features at multiple sites) or criterion 5 (contemporaneous and episodic formation of features over a large area). The relatively limited extent of exposure of older deposits in the study area cannot provide an amount of evidence comparable to that found for the Springfield event, for example, which is evidenced by multiple dikes at ten localities and shows a well-defined pattern over a distance of at least 22 miles (35 km) from the inferred energy center.

1.4.2.2 Locality SC 16

Locality SC 16 is approximately 2.5 miles northeast of Farmer City on Salt Creek. This Locality provided approximately 20 feet of intermittent exposure of a terrace that is approximately 8 feet above creek level. The stratigraphy measured down from the ground surface includes ~ 4 feet of very dark brown silty clay to clayey silt that grades downward into dark brown sandy gravel with clay. Maximum clast size in the sandy gravel is ~1 inch. Sandy gravel continues to a depth of 7 feet, where it sharply overlies bluish gray clayey silt that contains minor fine sand. A hand-auger hole revealed that this unit extends to at least 11 feet depth and coarsens downward, grading to sandy silt with clay and gravel at that depth. The entire unit is stiff to very stiff. The blue-gray color suggests that this silty unit is gleyed (reduced). The Soil Survey of De Witt County depicts the soil at this Locality as the Sawmill silty clay loam, a poorly drained soil that typically forms on flood plains that occasionally are flooded for brief periods from March through May.

This exposure is interpreted to be an overbank flood sequence and estimated to be middle to late Holocene in aged, based on the lack of significant soil development and lack of oxidation in the part near the modern water level (Table B-1-4).

This clayey silt unit is interrupted by two possible liquefaction features, Dikes 1 and 2 (Table B-1-4). Dike 1 extends from the water surface to the upper contact of the clayey silt (approximately 1 foot) and ranges from 1 to 1.5 inches wide. A bulbous protrusion extends laterally 6 inches from the main dike at the top of the clayey silt. Irregular pockets of clean sand in the overlying sandy gravel suggest that Dike 1 may continue upward through this

unit. The clayey silt observed for approximately 1 foot on either side of Dike 1 is black. The margins of this black clayey silt are sharp to very sharp.

Several characteristics suggest that Dike 1 represents a sudden injection originating from below: its side contacts are sharp and irregular; its width remains relatively constant with depth (over the short distance that could be observed); and it is filled with clean, medium- to coarse-grained gravelly sand. These characteristics are consistent with seismically induced features formed during liquefaction by hydraulic fracturing (Table B-1-3).

Dike 2 is a very thin (averaging ¼ inch wide), tabular fracture filled with clean, coarse-grained sand. The lack of clay in the fracture fill suggests that it may have resulted from liquefaction. The clayey silt found for approximately 1 foot on either side of Dike 2 is black. The margins of this black clayey silt are sharp to very sharp.

An approximately 12-foot-long section of the stream bank immediately downstream of Dike 2 has slumped, bringing grass and the uppermost brown silty clay down to stream level. This section overlies an ~ 1.5-foot-thick lens of gravelly sand with cobbles at the upper contact of the blue-gray clayey silt. The proximity of the slump block and Dike 2 suggests that Dike 2 may be related to the slumping, either because sand was dragged along the slide plane during slumping, or because the slumping resulted from liquefaction. The black clay surrounding Dike 2 could be interpreted as part of the slide plane. These interpretations do not, however, explain the presence of Dike 1 approximately 8 feet upstream.

The preferred explanation for Dikes 1 and 2 is that they both resulted from seismic liquefaction and are unrelated to bank slumping. The slump block at Locality SC 16 appears young (between a few months and a few years old), whereas Dikes 1 and 2 appear to be at least several hundred years old. The preferred interpretation for the origin of the black clayey silt surrounding both dikes is chemical alteration (oxidation?) by water flowing through the sandy dikes.

1.4.2.3 Locality SC 19/SC 18

Locality SC 19 lies approximately 1.5 miles northeast of Farmer City on Salt Creek. This locality includes approximately 100 feet of high-quality exposure that was as much as 6 feet high above stream level. The exposed sequence includes approximately 4.5 feet of predominantly clay to clayey silt overlying interbedded sand and silt that extend to the water surface and below. The Soil Survey of DeWitt County shows the soil at this site to be Sawmill silty clay loam, a poorly drained soil that typically forms on flood plains that occasionally are flooded for brief periods from March through May.

A general field description of the soil profile at Locality SC 19 includes a 0.3-foot-thick black A horizon overlying a dark brownish gray silty clay loam AB horizon that extends to a depth of 1.9 feet. Below this layer, a dark brownish gray blocky clay B_t horizon continues to a depth of 2.8 feet, followed by a red, structureless clay B_t horizon to a depth of 3.6 feet. Below this layer, a slightly weathered silty clay loam B horizon having a weak prismatic structure and very thin clay coatings on peds extends to a depth of 4.0 feet. A light-brownish gray silt loam C_{ox} horizon having abundant filled animal burrows extends to a depth of 4.7 feet, followed by medium-gray silt with sand lenses that continues below the water surface, which was at a depth of 5.8 feet.

This exposure is interpreted to be an overbank flood sequence, and its age estimated to be mid-Holocene based on its moderate degree of soil development and lack of deep oxidation near the modern water level (Table B-1-4).

The upper section of the exposure (the 4.5 feet of clay and clayey silt) represents a nonliquefiable cap. This cap is interrupted by two possible liquefaction features, Dikes 1 and 2 (Table B-1-4; Figure B-1-14). Both dikes are similar in size and shape, extending approximately 12 inches up from the interbedded sand and silt at the base of the exposure into the overlying silty clay loam. Both dikes reach a maximum width of 1.5 inches.

Several characteristics suggest that both Dikes 1 and 2 represent injection features. Their side contacts are sharp and irregular; they widen with depth; they are filled with clean fine- to medium-grained sand; the sand filling them fines upward; they include clayey silt clasts likely torn from their walls; and they extend upward from the sandy source material (in clear association with a source bed). These characteristics are consistent with those exhibited by seismically induced paleoliquefaction features (Table B-1-3).

Locality SC 18, located approximately 1,000 feet upstream of SC 19 on Salt Creek, includes approximately 15 feet of poor to moderate exposure that in places extends ~ 8 feet above stream level. The upper 4 to 5 feet of this exposure are covered with overhanging grasses and brush, which were not cleared. Below this section, a dark grayish brown silt loam extends to and below the water surface. The Soil Survey of DeWitt County, Illinois, maps Orion silt loam at this Locality. The Orion silt loam typically forms on floodplains that are somewhat higher than those where Sawmill soil is found, but that may be flooded for brief periods from March through May. The Orion silt loam typically includes a buried soil at an average depth of 38 to 40 inches.

This exposure is interpreted as an overbank flood sequence. Initially its age was estimated to be middle to late Holocene based on its lack of significant soil development and lack of oxidation in the part near the modern water level. However, dating of two radiocarbon samples from these deposits (7935_SC-19-2-1 and 7935_SC-19-2-2) yielded radiocarbon ages of 9,550 ± 40 yr BP and 10,230 ± 40 yr BP (Cal BC 9150 to 8750 and Cal BC 10,390 to 9780), respectively, suggesting the deposits are early Holocene (Table B-1-4; Exhibit 1).

Several irregular bodies of clean fine sand interrupt this sequence between 6 and 12 inches above the water level. The largest of these bodies reaches 3 inches in thickness and approximately 4 feet in length. These features may reflect liquefied injection, or may represent deformation of a fluvial sand lens, possibly due to sediment loading.

1.4.2.4 Locality M 6

Locality M 6 lies approximately 6 miles west of Colfax, Illinois, on the Mackinaw River. At this locality approximately 150 feet of continuous exposure that was approximately 12 feet in height above river level was found. The stratigraphy includes approximately 3 feet of soft clayey silt loess overlying 3.5 feet of loose fluvial sand, with a gravel lag at the base. These fluvial deposits rest unconformably on a thin (0.5- to 1-foot-thick) bed of very dense, fissile, oxidized, cross-bedded sandy silt. The fissile structure of this unit indicates that it was overridden by a glacier at some point. This sandy silt overlies a very hard, dark grayish brown, pebbly sandy clay till that was present down to the present water level of the river. Pebbles and cobbles, scattered sparsely throughout the till, sometimes reach 0.5 foot in

diameter. The Soil Survey of McLean County shows the soil at this Locality as Fox silt loam, a well-drained soil that typically forms from thin sheets of loess overlying sands and gravels on stream terraces.

A field description of the soil developed at this exposure includes 0.5 foot of a very dark grayish brown, friable, organic, silt loam A horizon at the surface, followed by a friable, grayish brown, silty clay loam BE horizon that extends to a depth of 0.9 feet, followed by a firm, dark yellowish brown, silty clay loam to a clay loam B_t horizon that has a weak, fine, prismatic structure that extends to the base of the loess at a depth of 3.2 feet. Below the loess, a friable, dark brown, sandy clay loam B_t horizon having a massive structure and abundant manganese oxide staining extends to 4.8 feet depth, followed by a friable, dark brown loamy sand that extends to the unconformity at the base of the fluvial deposits, at 6.4 feet depth. Below the unconformity, a firm, fissile, yellowish brown, oxidized, sandy clay loam C_{ox} horizon extends to a depth of 6.9 feet, followed by a hard, dark grayish brown pebbly sandy clay to clayey sand C horizon that extends to the base of the exposure at a depth of 10.5 feet.

Two prominent dikes intrude the till in the lower half of this exposure. Dike 1 comprises a vertical dike that reaches a maximum of 4 inches in width and strikes parallel to the bank exposure. A secondary dike extends outward in both directions from the southern (downstream) end of this dike, striking approximately perpendicular to the bank. This secondary part of Dike 1 reaches 2 inches in width and extends from near the water surface (~ 6 inches up) to approximately 2 feet above the main body of Dike 1 (approximately 5 feet in total length). Another secondary dike extends outward from Dike 1 toward and approximately perpendicular to the bank (resulting in an apparent vertical dip). This vertical part of Dike 1 can be traced for 4 feet up the bank exposure, until it is truncated by the dense, fissile sandy silt unit (Figure B-1-15A). This dike maintains a fairly constant width of 2 to 3 inches, with short (3- to 6-inch-long) branches extending outward from it (Figure B-1-15B). Dike 1 has very sharp, very irregular contacts and is filled with very fine- to medium-grained sand. The fill material is banded parallel to the walls of Dike 1, with bands defined by changes in grain size and color (caused by differences in the lithology of the sand grains).

A hand-auger hole advanced near Dike 1 showed that the silty clay till extends to a depth of at least 17.5 feet below ground surface at the top of the exposure (10.5 feet below the top of the till).

Dike 2 intrudes the till approximately 100 feet south of Dike 1. Like Dike 1, this dike reaches a maximum width of 4 inches and is truncated at its top by the dense, fissile sandy silt unit. Dike 2 is filled with medium-grained sand, has sharp contacts, and can be traced approximately 14 feet along and down the bank. This feature is tabular, strikes an approximately 20-degree angle to the bank exposure, and is vertical in cross section.

Both Dikes 1 and 2 exhibit several characteristics typical of seismic liquefaction features (Table B-1-3). Both clearly resulted from liquefied sand injected into the till from below. However, both Dikes 1 and 2 are truncated by the dense sandy silt deposit, which owes its fissile structure to compaction beneath a glacier. This relationship implies that both dikes were overridden by a glacier. Although clastic dikes commonly are formed by seismic liquefaction, they may also result from increased pore pressure, increased loading, drag,

and compression associated with the advance and deflation of glaciers (Broster, 1991; Dreimanis, 1992; Dreimanis and Rappol, 1997). Therefore, glaciotectonic deformation is as likely a cause for Dikes 1 and 2 at Locality M 6 as is seismic shaking.

1.4.3 Evidence for the Absence of Paleoliquefaction

Obermeier et al. (2001 and 2002) discuss the major factors that identify the severity of liquefaction and describe how to consider those factors when evaluating evidence for the presence or absence of strong shaking in a region. They note that throughout the meizoseismal area of a very strong earthquake, for which the Modified Mercalli Intensity (MMI) value is IX or higher, liquefaction features should abound even where liquefaction susceptibility is only moderate. Some dikes almost certainly exceeding 1 foot in width, and many smaller ones, should be discovered during a reasonably thorough search of the region. They suggest that in areas of moderate liquefaction susceptibility affected by earthquakes of MMI VII to VIII, small liquefaction features may be sparse, but should be numerous enough that some would be discovered during an examination of tens of miles of stream banks.

Moderate liquefaction susceptibility implies a medium relative density of the soil material, a water table within 10 to 15 feet of the surface, and a cap less than 25 to 30 feet thick (Obermeier et al., 2001 and 2002). A lower limit of moderate susceptibility requires a bed of silty sand, sand, or gravelly sand (generally less than about 40 percent gravel) that is at least 5 feet thick, capped by a minimum of approximately 1.5 feet of lower-permeability sediment. Where a cap is underlain by medium-grained sand or coarser sediment, the water table would have to be at or above the base of the cap at the time of the earthquake to produce liquefaction features. Otherwise, the high permeability of the material beneath the cap would permit dissipation of pore water pressure, leaving no evidence of paleoliquefaction. These authors, however, cite examples of liquefaction features produced from source beds much thinner than 10 feet in the meizoseismal zone of an ~ **M** 7 earthquake.

In the study area, deposits of latest Pleistocene and Holocene age were laid down by moderate to large streams and generally fit the criteria used to define moderate susceptibility. This level of susceptibility applies to stream deposits of both glaciofluvial braid-bar and Holocene point-bar origins. These deposits should have been at least moderately susceptible to liquefaction throughout the time since their deposition, with the possible exception of the hypsithermic period (middle Holocene; Obermeier, 1998), when the water table was several feet lower than in modern time. During our field reconnaissance, particular care was taken to identify and examine early Holocene and latest Pleistocene deposits. Exposures of pre-hypsithermic deposits were noted on field maps. In addition to the distinctive oxidation mottling observed at and below modern water levels, these deposits generally appeared to be more resistant to erosion than late Holocene deposits, forming a blockier appearance at and below the water level. Based on previous experience, Dr. Obermeier judged that even small clastic dikes would be visible in exposures of these deposits and that sufficient deposits were observed to document the absence of a Springfield-type event centered in the study region since the hypsithermic period (in the past 6 to 7 ka).

Deposits of latest Pleistocene age were noted on field maps if judged to have been moderately susceptible to liquefaction throughout much of the Holocene. Deposits at some localities likely pre-date the loess deposits at SC 25, which were intruded by clastic dikes (Table B-1-5). Evidence for the absence of paleoliquefaction features at these localities is described in Table B-1-5; the locations of the localities are shown on Figure B-1-6. The reported absence of paleoliquefaction features in the Mahomet gravel pits (Locality S 14; Figure B-1-16) offers the strongest evidence for the absence of significant ground shaking in this part of the study region. The limited number and small extent of the exposures of late Pleistocene fluvial and loess deposits observed elsewhere in the region make it more difficult to evaluate the significance of the features observed at SC 25. However, no evidence comparable to that produced by the Springfield event—the multiple dikes at ten localities and a well-defined regional pattern over an area 22 miles (35 km) in diameter – was found.

1.4.4 Conclusions

Field reconnaissance conducted for this study obtained additional information regarding the prehistoric record of earthquakes within the near region (approximately 25- to 30-mile radius) of the EGC ESP Site. That information is summarized below.

1. No evidence for a post-hypsithermic (post-mid-Holocene) earthquake comparable to the postulated Springfield event (McNulty and Obermeier, 1999) was observed in the study area. Sufficient exposures of pre-hypsithermic (> 6 to 7 ka) deposits were observed to demonstrate the absence of paleoliquefaction features indicative of an energy source for a comparable event (estimated **M** 6.2 to 6.8) in the site vicinity. Radiocarbon ages from samples originally estimated to be mid-Holocene yielded ages of approximately 10 ka (see Section 4.2.3), suggesting that the absence of significant events may extend back even further into the early Holocene.

2. Isolated features of mid-Holocene and latest Pleistocene/early Holocene age were observed in the study area that could be interpreted as evidence of seismically induced paleoliquefaction. Features of probable mid- to early Holocene age were observed at two localities along Salt Creek (SC 16 and SC 19/SC 18), approximately 1.5 to 2.5 miles northeast of Farmer City and approximately 11.5 to 13 miles from the EGC ESP Site. Characteristics of the dikes exposed at these locations are consistent with seismic liquefaction features. Assuming that these features are seismically induced, their small scale and the lack of evidence for similar features elsewhere in the study area suggest either a more distant source or a low-magnitude event (at or close to threshold of paleoliquefaction, estimated to be MMI VI or VII). Radiocarbon ages for samples from Locality SC 19 indicate that these features formed after 9550 ± 40 yr. BP (CAL BC 9150 to 8750).

3. Older features (clastic dikes that cut the post-glacial silt cap [probably early post-glacial loess deposits]) were observed at Locality SC 25, approximately 5.5 miles northeast of Farmer City and approximately 17 miles from the EGC ESP Site. Those features post-date loess deposits estimated to be ~ 16 to 17 ka. Based on weathering and soil development of the clastic dikes and silt cap, and the height

of the water table at the time of formation (~ 3 feet higher than at present), the dike features are inferred to be latest Pleistocene to early Holocene (< 17 to 10 ka). Sedimentary and stratigraphic characteristics of host deposits and material sources, as well as conduit morphology, are consistent with a seismic origin for these features. It is estimated that, if seismically triggered, clastic dikes observed at this location would imply Modified Mercalli Intensity values of at least VII to VIII.

4. Clastic dikes observed in till deposits at Locality M 6, approximately 29 miles north-northeast of the EGC ESP Site, appear to have formed during the latest glacial advance in that region (~ 17.7 ± 1 ka). The event that triggered injection of the clastic dikes at this location is uncertain. Both dewatering related to glacial processes and seismic shaking are possible mechanisms.

5. No evidence for paleoliquefaction of an age similar to that observed at Locality SC 25 was identified at any other locality, although the possibility that clastic dikes at Locality M 6 formed contemporaneously with the features at Locality SC 25 cannot be precluded at this time given the uncertainties in age estimates. The limited extent of exposure of older deposits makes it difficult to document the well-defined regional pattern needed to estimate a magnitude and location for this event. Susceptible deposits of estimated latest Pleistocene age at Localites M 2, S 6, S 14, and NSC 1 show evidence for no liquefaction. These localities should have been favorable sites for liquefaction throughout much of the latest Pleistocene and Holocene, with the possible exception of NSC 1, where the fluvial deposits may not have been below the water table throughout the Holocene. Deposits at these sites therefore provide reasonable evidence for the absence of significant ground shaking since latest Pleistocene/early Holocene time, and may limit the geographic extent of liquefaction that can be correlated with the features observed at Locality SC 25. The extensive Mahomet gravel pit exposures (S 14), in particular, provide evidence for the absence of strong ground motion that would produce significant liquefaction since deposition of the upper silt approximately 17 to 18 ka.

The results of this study suggest that there have been no repeated moderate- to large-magnitude (comparable to the postulated Springfield-type) events in the vicinity of the EGC ESP Site in latest Pleistocene to Holocene time. The late Holocene record in particular is sufficient to demonstrate the absence of such events in the past approximately 6 to 7 ka. The significance of the latest Pleistocene/early Holocene features recorded at Locality SC 25 is less certain. There is insufficient information to accurately estimate a location or magnitude for a postulated seismic source. The features, however, suggest that the range of maximum magnitude assigned to a random background earthquake in the probabilistic seismic hazard analysis for the EGC ESP Site should include events comparable to that estimated for the Springfield earthquake (i.e., **M** 6.2 to 6.8).

CHAPTER 2

References

Atkinson, G.M. and D.M. Boore. "Some Comparisons between Recent Ground-Motion Relations." *Seismological Research Letters*. Vol. 68, No. 1. pp. 24-40. 1997.

Bauer, R.. Illinois Geological Survey. Personal Communication. November 21, 2002.

Broster, B.E. "Glaciotectonic Deformation in Sediment and Bedrock, Hat Creek, British Columbia." *Geographie Physique et Quaternaire.* Vol. 45, No. 1. pp. 5-20. 1991.

Campbell, K.W. Development of Semi-Empirical Attenuation Relations for the CEUS, USGS Annual Technical Summary. Available: http://erp-web.er.usgs.gov/reports/annsum/vol43/ni/g0011.pdf. 2001.

Chester, J. S., and M.P. Tuttle. "Paleoseismology in the Cache River Valley, Southern Illinois." *Technical Progress Report Submitted to U.S. Geological Survey National Earthquake Hazards Reduction Program*. U.S.G.S. External Grant Nos. 1434-HQ-98-GR-00013 and 1434-HQ-98-GR-00015. 2000.

Dreimanis, A. "Downward Injected Till Wedges and Upward Injected Till Dikes," in Robertson, A.M., M., B. Ringberg, U. Miller, and L. Brunnberg (eds.). *Quaternary Stratigraphy, Glacial Morphology, and Environmental Changes*. Geological Survey of Sweden Research Paper. Serie Ca81. pp.91-96. 1992.

Dreimanis, A., and M. Rappol. "Late Wisconsinan Sub-Glacial Clastic Intrusive Sheets along Lake Erie Bluffs, at Bradtville, Ontario, Canada." *Sedimentary Geology*. Vol. 111. pp. 225-248. 1997.

Folmer, Leon. Illinois Geological Survey. Personal Communication. October 4, 2002.

Folmer, Leon. Illinois Geological Survey. Personal Communication. October 15, 2002.

Green, R.A. *Energy-Based Evaluation and Remediation of Liquefiable Soils*. Ph.D. Dissertation. Virginia Polytechnic Institute and State University. 394 pp. 2001.

Green, R.A., S.F. Obermeier, and S.M. Olson. "The Role of Paleo-Liquefaction Studies in Performance-Based Earthquake Engineering in the Central-Eastern United States." 13th World Conference on Earthquake Engineering, Vancouver, BC, Canada. Paper No. 1643. 14 p. Available at: <http://wwwpersonal.engin.umich.edu/~rugreen/papers/WCEE.pdf>. August 1-6, 2004a.

Green, R.A., S.F. Obermeier, and S.M. Olson. "Geotechnical Analysis of Paleoseismic Shaking Using Liquefaction Features: Part II. Field Examples." Report No. UMCEE04-08. Department of Civil and Environmental Engineering, University of Michigan, Ann Arbor, MI. Available at: <http://www.personal.engin.umich.edu/~rugreen/papers/UMCEE0408.pdf>. 2004b.

Hajic, E.R., and M.D. Wiant. "Dating of Prehistoric Earthquake Liquefaction in Southeastern and Central Illinois." *Illinois State Museum Society*. Report to the U.S. Geological Survey. 57 pp. 1997.

Hajic, E.R., M.D. Wiant, and J.J. Oliver. "Distribution and Dating of Prehistoric Earthquake Liquefaction in Southeastern Illinois, Central U.S." Final Technical Report Submitted to the U. S. Geological Survey National Earthquake Hazards Reduction Program. Contract No. 1434-93-G-2359. 33 pp. 1995.

Hansel, A.K., and W.H. Johnson. "Wedron and Mason Groups: Lithostratigraphic Reclassification of Deposits of the Wisconsin Episode, Lake Michigan Lobe Area." *Department of Natural Resources Illinois State Geological Survey Bulletin*. Vol. 104. 116 pp. 1996.

Harrison, R.W., and A. Schultz. "Tectonic Framework of the Southwestern Margin of the Illinois Basin and its Influence on Neotectonism and Seismicity." *Seismological Research Letters*. Vol. 73, No. 5. pp. 698-731. 2002.

Hildenbrand, T. G., J. H. McBride, and D. Ravat. The Commerce Geophysical Lineament and its Possible Relation to Mesoproterozoic Igneous Complexes and Large Earthquakes in the Central Illinois Basin. *Seismological Research Letters*. Vol. 73, No. 5, pp. 640-659. 2002.

Illinois State Geological Survey. Structural Features in Illinois: Line Features (Axial or Flexure) of Anticlines, Synclines and Monoclines: ISGS GIS Database *path_name_suppressed*/structclines, Illinois State Geological Survey, Champaign, IL. 1995. Available: http://www.isgs.uiuc.edu/nsdihome/outmeta/structclinesf.html. [08.08.2002]

Indiana Geological Survey. Structural_Features_SW: Structural Features of Southwestern Indiana (Indiana Geological Survey, Line Shapefile). 2001. Available: http://igs.indiana.edu/arcIMS/southwest/Metadata/Structural_Features_sw.html. [29.05.2003].

Lineback, J.A. "Quaternary Deposits of Illinois." Illinois State Geological Survey Map, scale 1:500,000. 1979.

McNulty, W.E., and S.F. Obermeier. "Liquefaction Evidence for at least Two Strong Holocene Paleoearthquakes in Central and Southwestern Illinois, USA." *Environmental and Engineering Geoscience*. Vol. 5, No. 2. pp. 133-146. 1999.

Munson, P.J., S.M. Obermeier, C.A. Munson, and E.R. Hajic. "Liquefaction Evidence for Holocene and Latest Pleistocene in the Southern Halves of Indiana and Illinois—a Preliminary Overview." *Seismological Research Letters*. Vol. 68, No. 4. pp. 523-536. 1997.

Nelson, W.J. *Structural Features in Illinois*. Illinois State Geological Survey Bulletin 100. 144 pp. 1995.

Obermeier, S.F. "Using Liquefaction-Induced Features for Paleoseismic Analysis." in McCalpin, J.P. (ed.). *Paleoseismology*. Academic Press Inc., San Diego. pp. 331-396. 1996.

Obermeier, S.F. "Liquefaction Evidence for Strong Earthquakes of Holocene and Latest Pleistocene Ages in the States of Indiana and Illinois, USA." *Engineering Geology*. Vol. 50. pp. 227-254. 1998.

Obermeier, S.F., U. S. Geological Survey, Emeritus, Reston, Virginia; EqLiq Consulting. Written (electronic mail) Communication to Kathryn Hanson. January 10, 2003.

Obermeier, S.F., U. S. Geological Survey, Emeritus, Reston, Virginia; EqLiq Consulting. Written (electronic mail) Communication to Kathryn Hanson. May 13, 2003.

Obermeier, S.F., U. S. Geological Survey, Emeritus, Reston, Virginia; EqLiq Consulting. Personal Communication. August 9, 2003.

Obermeier, S.F., N.K. Bleuer, C.A. Munson, P.J. Munson, W.S. Marin, K.M. McWilliams, D.A. Tabaczynski, J.K. Odum, M. Rubin, and D.L. Eggeert. "Evidence of Strong Earthquake Shaking in the Lower Wabash Valley from Prehistoric Liquefaction Features." *Science*. Vol. 251. pp. 1061-1063. 1991.

Obermeier, S.F., J.R. Martin, A.D. Frankel, T.L. Youd, P.J. Munson, C.A. Munson, and E.C. Pond. "Liquefaction Evidence for One or More Strong Holocene Earthquakes in the Wabash Valley of Southern Indiana and Illinois, with a Preliminary Estimate of Magnitude." *U.S. Geological Survey Professional Paper 1536*. 27 pp. 1993.

Obermeier, S.F., E.C. Pond, and S.M. Olson, with contributions by Green, R.A., T.D. Stark, and J.D. Mitchell. "Paleoliquefaction Studies in Continental Settings: Geologic and Geotechnical Factors in Interpretations and Back-Analysis." *U.S. Geological Survey Open-File Report 01-29*. 75 pp. 2001.

Obermeier, S.F., Pond, E.C., Olson, S.M, and Green, R.A. "Paleoliquefaction Studies in Continental Settings." in Ettensohn, F.R., N. Rast, and C.E. Brett (eds.). *Ancient Seismites*. Boulder, Colorado. *Geological Society of America Special Paper 359*. pp. 13-27. 2002.

Olson, S.M., R.A. Green, and S.F. Obermeier. "Geotechnical Analysis of Paleoseismic Shaking Using Liquefaction Features: Part I. Major Updating of Analysis Techniques." U. S. Geological Survey Open-File Report 03-307. 33 pp. 2003. Version 1.1 available at: http://pubs.usgs.gov/of/2003/of03-307.pdf. Revised January 30, 2004.

Pond, E.C., and J.R. Martin. "Estimated Magnitudes and Accelerations Associated with Prehistoric Earthquakes in the Wabash Valley Region of the Central United States." *Seismological Research Letters*. Vol. 68, No. 4. pp. 611-623. 1997.

Somerville, P., N. Collins, N. Abrahamson, R. Graves, and C. Saikia. "Ground Motion Attenuation Relations for the Central and Eastern United States." Final Report to U.S. Geological Survey. 2001.

Su, W.J., and J.H. McBride. *Final Technical Report – Study of a Potential Seismic Source Zone in South-Central Illinois (abs.)*. Technical Report Submitted to the U.S. Geological Survey under USGS External Grant Number 99HQGR0075. 1999.

Toro, G., N. Abrahamson, and J. Schneider. "Model of Strong Ground Motions from Earthquakes in the Central and Eastern North America: Best Estimates and Uncertainties." *Seismological Research Letters*. Vol. 68, pp. 41-57. 1997.

Tuttle, M.P. "The Use of Liquefaction Features in Paleoseismology: Lessons Learned in the New Madrid Seismic Zone, Central United States." *Journal of Seismology*. Vol. 5. pp. 361-380. 2001.

Tuttle, Martitia P. M. Tuttle & Associates. Written (Electronic) Communication. February 11, 2003.

Tuttle, M.P., J. Chester, R. Lafferty, K. Dyer-Williams, and R. Cande. "Paleoseismology Study Northwest of the New Madrid Seismic Zone." *U.S. Nuclear Regulatory Commission Report NUREG/CR-5730*. 96 pp. 1999.

University of Missouri, 1991. Department of Geology. State Geologic Faults of Missouri. Available: http://msdis.missouri.edu/html/sfault.html. [15.08.2002].

Wheeler, R.L., and C.H. Cramer. "Updated Seismic Hazard in the Southern Illinois Basin: Geological and Geophysical Foundations for Use in the 2002 USGS National Seismic-Hazard Maps." *Seismological Research Letters*. Vol. 73, No. 5. pp. 776-791. 2002.

TABLE B-1-1

LIQUEFACTION EVIDENCE FOR PREHISTORIC EARTHQUAKES IN THE SOUTHERN ILLINOIS BASIN

Seismic Hazards Report for the EGC ESP Site

Name of Earthquake(s)	Location	Size and Distribution of Features	Age[1]	Estimated Magnitude	Reference(s)
Lower Wabash Valley					
Vincennes-Bridgeport	~ 15 miles (25 km) west of Vincennes, Indiana	≥ 0.5-m dike width; 150-km maximum distance from inferred energy center	~ 6,100 ± 200 yr. BP	≥ **M** 7.5 to 7.8 (magnitude-bound, cyclic stress, and energy-stress methods)	Munson et al. (1997); Obermeier (1998); Obermeier et al. (1993);
				M 7.7 to 7.8 (energy-stress) (see comments below by S. Obermeier, 10 January, 2003 and 13 May, 2003	Pond and Martin (1997)
				M ~7.2-7.3 (based on revised CEUS magnitude-bound relation	Olson et al. (2005, in press)

TABLE B-1-1

LIQUEFACTION EVIDENCE FOR PREHISTORIC EARTHQUAKES IN THE SOUTHERN ILLINOIS BASIN

Seismic Hazards Report for the EGC ESP Site

Name of Earthquake(s)	Location	Size and Distribution of Features	Age[1]	Estimated Magnitude	Reference(s)
				M 7.0+ to 7.5 (cyclic stress method using site-specific geotechnical data and most recent magnitude scaling factors, suggested by E. Idriss and L. Youd) **M** ~7.5 (2003 reanalysis using energy-based solution and NEHRP recommended procedures for calculating ground motions)	Green et al., (2004a, 2004b)
				The energy-stress method used by Pond and Martin (1997) is flawed (energy attenuation relations used should not be used for liquefaction analysis) and the results are not reliable.	S. Obermeier (personal communication, 13 May 2003); Green et al., (2004a, 2004b)
Skelton-Mt. Carmel	~ 25 miles (40 km) southwest of Vincenees, Indiana	≥ 0.5-m dike width; 50- to 60-km maximum distance from inferred energy center	~ 12,000 ± 1,000 yr. BP	**M** 7.1 to 7.2 (magnitude-bound); **M** 7.3 (energy-stress) **M**6.7 (based on revised CEUS magnitude-bound relation	Munson et al. (1997); Pond and Martin (1997); Hajic and Wient (1997); Obermeier (1998); Olson et al. (2005, in press)

TABLE B-1-1

LIQUEFACTION EVIDENCE FOR PREHISTORIC EARTHQUAKES IN THE SOUTHERN ILLINOIS BASIN

Seismic Hazards Report for the EGC ESP Site

Name of Earthquake(s)	Location	Size and Distribution of Features	Age[1]	Estimated Magnitude	Reference(s)
Single site near Iona, Indiana	22 miles (35 km) southeast of Vincennes, Indiana, near Iona (location not shown on Figure B-1-2)	Very small and restricted (probably limited to 5 km)	4,000 ± 500 yr. BP	Near threshold (**M** ~5.5 – 6.0 to < 6.7)	Munson et al. (1997); Obermeier (1998)
Central and Southern Indiana					
Vallonia	East Fork valley ~ 60 miles (100 km) east of the Wabash Valley seismic zone	≥ 0.5 m; 36 km maximum distance from inferred energy center	3,950 ± 250 yr. BP	**M** ≥ 6.9 (magnitude-bound) **M** 7.1 (energy-stress) **M** 6.3 (new magnitude-bound relation)	Munson et al. (1997); Obermeier (1998); Pond and Martin (1997) Olson et al. (2005, in press)
Martinsville-Waverly	~ 18 to 30 miles (30 to 50 km) southwest of Indianapolis, Indiana (location poorly constrained)	≥ 0.15 to ≤ 0.5 m; 28 km maximum distance from inferred energy center	Between 8,500 and 3,500 yr. BP	**M** 6.8 (magnitude-bound); **M** 6.9 (energy-stress) **M** 6.2 (new magnitude-bound relation)	Munson et al. (1997); Obermeier (1998) Geotechnical analyses demonstrate that these features are not associated with the **M** ~ 7.5 Vincennes earthquake Olson et al. (2005, in press)
Single site near Elnora, Indiana	37 miles (60 km) east-northeast of Vincennes (location not shown on Figure B-1-2)	Limited areal extent	2,000 ± 500 yr. BP	**M** ≥ 5.5 to 6.0	Munson et al. (1997); Obermeier (1998)
Single site along Indian Creek, Indiana	~ 30 mi (50 km) south-southwest of Indianapolis (location not shown on Figure B-1-2)	Single site	~ 20,000 yr. BP	Unknown	Munson et al. (1997); Obermeier (1998)

TABLE B-1-1

LIQUEFACTION EVIDENCE FOR PREHISTORIC EARTHQUAKES IN THE SOUTHERN ILLINOIS BASIN

Seismic Hazards Report for the EGC ESP Site

Name of Earthquake(s)	Location	Size and Distribution of Features	Age[1]	Estimated Magnitude	Reference(s)
Ohio River region—Absence of paleoliquefaction in Ohio River sediments along the Indiana-Kentucky and Illinois-Kentucky borders suggests that this area has not experienced severe ground shaking in the past 4,500 years (Munson et al., 1997). However, those authors suggest that a 5- to 6-m-thick clay cap may have kept sand dikes from penetrating to levels above the current maintained water level of the Ohio River.					

Name of Earthquake	Location	Size and Distribution of Features	Timing[1]	Estimated Magnitude	Reference
Central and Southern Illinois					
Springfield	~ 22 miles (35 km) northeast of Springfield, Illinois	Maximum dikes width 0.4 m; 35 km maximum distance from inferred energy center	One, possibly two, events between 5900 and 7400 yr. BP	**M** 6.2 to 6.8 **M** 5.5 (second event) **M** 6.3 (based on revised magnitude-bound relation)	Hajic et al. (1995); McNulty and Obermeier (1999) Olson et al. (2005, in press)
Shoal Creek	Centered in vicinity of lower Shoal Creek near its confluence with Kaskaskia River: ~ 40 miles (65 km) east-southeast of St Louis, Missouri. Alternative location: Centralia fault (Du Quoin monocline)	Maximum dike width 1.55 m; 35 km maximum distance from inferred energy center	~ 5670 ± 80 yr. BP (4520 ± 160 BC or 6500 yr. BP)	**M** 6.5 (lower limit) **M** 6.3 (based on revised magnitude-bound relation)	McNulty and Obermeier (1999); Tuttle et al. (1999) Olson et al. (2005, in press)
Cache River	Cache River from Sandusky to the Mississippi River	Dike width 1 to 9 cm	Two ages: maximum age AD 1020 to 1250 for younger and possibly older event(s)	Unknown	Chester and Tuttle (2000)

TABLE B-1-2

SUMMARY OF DEPOSITS IN BANK EXPOSURES

Seismic Hazards Report for the EGC ESP Site

River	Salt Creek	Sangamon	Mackinaw
Total distance observed	11.7 miles	12.3 miles	17.5 miles
Estimated total length of till observed	150 feet	4,950 feet	8,200 feet
Estimated total length of liquefiable latest Pleistocene alluvium observed (glaciofluvial outwash)	360 feet	135 feet	440 feet
Estimated total length of pre-hypsithermic (early Holocene) alluvium observed	1,200 feet	2,000 feet	5,850 feet

Notes:

1. Limited reconnaissance (approximately 1 mile walked) on the North Fork of Salt Creek revealed ~ 20-foot exposure of latest Pleistocene alluvium.
2. Sections of riverbank not accounted for in this table generally consist of younger Holocene terrace deposits. Approximately 70 to 80 percent of the riverbanks observed were covered.
3. The estimated total lengths of liquefiable latest Pleistocene alluvium shown in this table do not include the exposures at Locality S 14 (the Mahomet gravel pit).

TABLE B-1-3

CRITERIA FOR DIFFERENTIATING ORIGINS OF LIQUEFACTION FEATURES

Seismic Hazards Report for the EGC ESP Site

	SC 25	SC 16	SC 18	SC 19	M 6
Seismic					
Dike widens at depth or remains constant in width (injected from below)	Yes	Yes	No	Yes	Yes?
Dike fill includes silty sand, clean sand, or gravelly sand (liquefiable material)	Yes	Yes	Yes	Yes	Yes
Dike fill fines upward or remains constant in grain size (injected from below)	Yes	No	N/A	Yes	Yes
Dike is tabular in plan view	Yes	Yes	No	Yes?	Yes
Dike wall contacts are sharp and planar or irregular (injected suddenly)	Yes	Yes	Yes	Yes	Yes
Dike is observed in clear association with source material	Yes	No	No	Yes	No
Source material is observed to be loose	Yes	N/a	N/A	Yes	N/A
Source material is located at or below the water table	Yes	Yes?	Yes?	Yes	Yes?
Nonliquefiable cap present	Yes	Yes	Yes	Yes	No
Evidence of recurrent events is found nearby	Yes	Yes	Yes	Yes	No
Dike fits a regional pattern based on dike width and abundance	No[i]	No[ii]	No[ii]	No[ii]	No[i]
Glaciotectonic					
Evidence of basal drag, ice push, meltwater expulsion, and hydraulic fracturing is found					
Temporal association with glaciers	No	No	No	No	Yes
Spatial association with glaciers	No	No	No	No	Yes
Associated or nearby evidence for subglacial deformation of soft-sediments	No	No	No	No	Yes
Terminates at base of overlying till	No	No	No	No	Yes
Other Nonseismic Mechanisms					
Artesian conditions are recorded historically in the vicinity	No	No	No	No	No
Dike is located in a setting prone to artesian conditions (e.g., at the base of a hill or near an artificial levee)	No	No	No	No	No
Dike is associated with features that may indicate nonseismic landsliding	No	Yes	No	No	No

[i] The paucity of latest Pleistocene to early Holocene deposits identified during this field investigation makes it difficult to assess this parameter. The absence of evidence for liquefaction was noted at several locations in the study area (Table B-1-5).

TABLE B-1-3

CRITERIA FOR DIFFERENTIATING ORIGINS OF LIQUEFACTION FEATURES

Seismic Hazards Report for the EGC ESP Site

[ii] The proximity of the three sites where possible mid-Holocene liquefaction features are recognized (SC 16, SC 18, and SC 19) and the small scale of the features at all sites do not define a clear regional pattern for a mid-Holocene event centered in the EGC ESP Site area. Sufficient exposures of pre-hypsithermic deposits throughout the area are available to demonstrate the absence of larger late Holocene liquefaction features in the site vicinity.

TABLE B-1-4

CHARACTERISTICS AND ESTIMATED AGES OF POTENTIAL LIQUEFACTION FEATURES IDENTIFIED IN SITE VICINITY

Seismic Hazards Report for the EGC ESP Site

Locality	Coordinates	No. of dikes	Maximum Width		Material Intruded	Interpretation	Estimated Age
			in.	cm			
Salt Creek SC 25	365962 E 4460489 N	6	4	10	Silt cap (loess)	Preferred origin for dikes is seismic liquefaction.	Latest Pleistocene/early Holocene based on weathering of dike material, soil development, and estimation of paleo-water table levels.
Salt Creek SC 16	363816E 4459593N	2	1.5	4	Clayey silt (fluvial)	Dikes likely caused by seismic liquefaction.	Mid- to late Holocene based on soil development.
Salt Creek SC 19/ SC 18	363376E 4457299N	2	1.5	4	Clayey silt (fluvial)	Preferred origin for dikes is seismic liquefaction. Sill may indicate seismic liquefaction or soft sediment deformation.	Mid- to late Holocene based on soil development.
Mackinaw River M 6	355764E 4493685N	2	4	10	Lodgement till	Origin for dikes is uncertain; may be seismic or glaciotectonic fluidized injection.	Latest Pleistocene (17.7 ± 1 ka) capped by glacially compacted fluvial deposits.

Note: Coordinate system is UTM (meters) zone 16, NAD 83.

TABLE B-1-5

LOCALITIES OF OLDER ALLUVIUM

Seismic Hazards Report for the EGC ESP Site

Locality	Coordinates	Unit Description	Estimated Age	Comments
Sangamon River				
S 2	368766E 4476983N	Silt cap (~ 5 feet thick) overlying oxidized pebbly gravelly sand (fluvial)	Middle Holocene	Good exposure (~50 feet) having no apparent liquefaction features or fractures.
S 3	368874E 4476926N	Older alluvium overlying till, overlain by ~ 6-foot-thick silt cap at upstream end of exposure	Pre-hypsithermic (early Holocene)	No liquefaction features observed. Good conditions for liquefaction, but limited exposure.
S 6	383748E 4454301N	Silt cap (~2 feet thick) overlying ~10 feet of interbedded gravelly sand, sand, and silt (fluvial)	Latest Pleistocene to early Holocene. Based on weathering and soil development, this unit is estimated to be equivalent in age to SC 25 or perhaps older. Radiocarbon analysis of charcoal from deposit (sample 7935_S-6-2) yielded a radiocarbon age of 35,550 ± 1,200 yr. BP. This age suggests the charcoal was re-used from an earlier time and does not represent the age of the deposit	Contact between silty clay to clayey silt unit and underlying coarse sand exposed for 40 feet. The sand below the fine-grained unit, which lies ~ 2 to 3 feet above present water level, should have been below the water table at the time of the SC 25 event (comparable age and position). There is good evidence for the absence of liquefaction in susceptible deposits at this site.
S 8	No reading taken at this location (see Figure B-1-6)	Fine-grained alluvium (~ 9 to 10 feet thick)	Middle Holocene	No liquefaction observed along 30-foot-long exposure. Larger paleoliquefaction features should have been apparent.
S 9	383723 E 4453574 N	20-foot-high stream bank: interbedded loess and water-laid fine sediment (~ 12 feet thick) overlying thin gravelly sand, silt, and poorly sorted gravel (~ 8 feet thick)	This unit appears to be older than S 6 or SC 25 based on geomorphic position and soil development (shown on Soil Survey map as soil unit 570C2)	The exposure at this site is poor, covered by slump colluvium and vegetation.

TABLE B-1-5

LOCALITIES OF OLDER ALLUVIUM

Seismic Hazards Report for the EGC ESP Site

Locality	Coordinates	Unit Description	Estimated Age	Comments
S 9	383723 E 4453574 N	20-foot-high stream bank: interbedded loess and water-laid fine sediment (~ 12 feet thick) overlying thin gravelly sand, silt, and poorly sorted gravel (~ 8 feet thick)	This unit appears to be older than S 6 or SC 25 based on geomorphic position and soil development (shown on Soil Survey map as soil unit 570C2)	The exposure at this site is poor, covered by slump colluvium and vegetation.
Sangamon River				
S 10	382937E 4452756N	14- to 15-foot-high stream bank: silt cap (3 to 5 feet thick) overlying gravelly sand	Latest Pleistocene to early Holocene	Poor exposures of terrace deposits along meander loop. Exposures (~ 300-foot-long) insufficient to assess presence/absence of paleoliquefaction.
S 11	382525E 4452432N	9-foot-high stream bank: alluvium	Pre-hypsithermic (early Holocene)	~ 200 feet of exposure. Very good evidence of no liquefaction in susceptible deposits.
S 12	no reading taken at this location	~ 20-foot-high stream bank: gravel observed up at least half the bank	Latest Pleistocene/early Holocene based on geomorphic position.	Stream bank mostly covered. No information observed regarding presence/absence of paleoliquefaction.
S 13	379041E 4449465N	9-foot-high terrace: silt cap (4 to > 9 feet thick) overlying strongly oxidized fluvial deposits (clean, medium-grained sand)	Pre-hypsithermic (early Holocene)	~ 100 feet of good exposure (left bank adjacent to a rifle range) of susceptible deposits showing no evidence of liquefaction.

TABLE B-1-5

LOCALITIES OF OLDER ALLUVIUM

Seismic Hazards Report for the EGC ESP Site

Locality	Coordinates	Unit Description	Estimated Age	Comments
S 14	379879E 4449215N	Upper section: glacial outwash (cross-bedded sand and pebbly gravel) overlies 4-foot-(average) to 6-foot-(locally)-thick silt bed (slackwater deposit), which overlies glacial outwash (sand and gravel)	Slackwater deposit in upper part of section is correlated to flooding event (breaching of the Bloomington moraine at Saybrook) ~ 17 to 18 ka.	Prairie material gravel pit (Mahomet Operation,Yard 58). Excavation started in 1971. Gravel pit is > 70 feet deep, covers ~ 150 acres. 100+ acres of continuous exposure observed since operation began. Upper section well exposed in older part of gravel pit. Present water table is just below floor of older gravel pit (probably within a few feet of base of silt layer). Lack of oxidation observed in deposits below silt layer suggests water table generally has been relatively high since deposition. No anomalous features (clastic dikes, fractures) in silt layer noted during excavation. Site conditions are very susceptible to liquefaction, providing good evidence for lack of significant paleoliquefaction since deposition of the silt layer.
Mackinaw River				
M 2	361731E 4491708N	Older alluvium (stratified sand) underlying 7- to 8-foot-high terrace that onlaps hill, underlain by poorly sorted gravelly sand unit having subvertical filled fractures and deformation features	Based on geomorphic position and soil profile development, the fluvial deposits underlying the terrace probably are latest Pleistocene in age.	Deformation features observed in poorly sorted sand unit are likely related to glaciotectonic or periglacial (frost-wedge) processes. The hummocky terrain associated with these deposits suggests the deposits are ice-contact drift or ablation till (deposited during stagnating ice conditions). The overlying fluvial deposits appear to be only slightly younger based on the soil profile developed across the contact. These deposits, which would be susceptible to liquefaction, show good evidence of no disruption (paleoliquefaction) since deposition.
M 3	360046E 4492330N	~ 10-foot-high terrace: silt cap (4 feet thick) overlies fluvial sand and gravel (4.5 feet thick); which overlies? silt (2 feet thick)	Pre-hypsithermic (early Holocene)	25-foot long exposure showing good evidence of no paleoliquefaction in susceptible deposits.

TABLE B-1-5

LOCALITIES OF OLDER ALLUVIUM

Seismic Hazards Report for the EGC ESP Site

Locality	Coordinates	Unit Description	Estimated Age	Comments
Mackinaw River				
M 101	351920E 4495543N	10-foot-high terrace: silt cap (9 to 11 feet thick) overlies gravel	Pre-hypsithermic (early Holocene)	20–foot-long exposure showing good evidence of no paleoliquefaction in susceptible deposits.
M 102	350494E 4496546N	Alluvium	Pre-hypsithermic (early Holocene)	Good 60-foot-long exposure showing no evidence of paleoliquefaction. Deposits probably not as old as those at SC 25. Additional 200 feet of good exposure downstream showing no evidence of paleoliquefaction.
Additional exposures of pre-hypsithermic deposits noted on field maps				No evidence of significant paleoliquefaction features or anomalies noted during visual examination of these exposures from canoe.
Salt Creek				
SC 21	361929.6 4456133	12-foot-high terrace: 5-foot-thick silt cap overlies 7 feet of fluvial sand and gravel (glacial outwash)	Latest Pleistocene	Approximately 30 feet of poor to moderate exposure. Sediments probably would have liquefied, although features may not have been preserved in the relatively thick silt cap.
North Fork Salt Creek				
NSC 1	350937E 4464273N ~ 500 feet upstream of confluence with West Fork of North Salt Creek	11-foot-high terrace: thin silt cap (2 feet thick) overlies fluvial deposits (glacial outwash) (~ 8.5 feet thick), which overlies 1 to 2 feet of till at base of exposure	Latest Pleistocene	20+ feet of exposure. Sediments would have liquefied if water table were 2+ feet higher than at present. It might be difficult to see small clastic dikes in these coarse sands. No larger dikes or anomalous features observed. These deposits are likely old enough and in a favorable position in relation to the water table to have recorded the SC 25 event.

Note: Coordinate system is UTM (meters) zone 16, NAD 83.

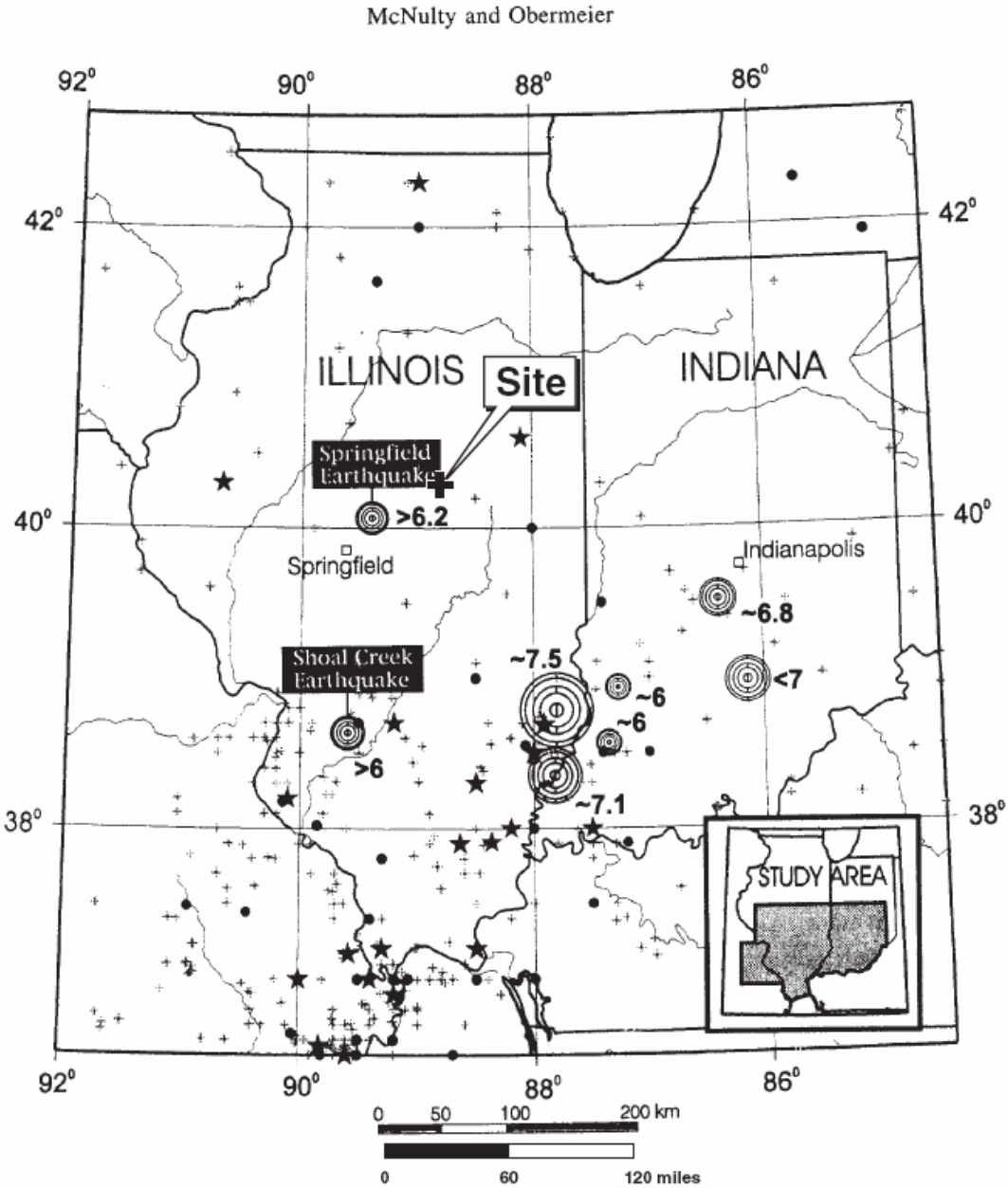

A star represents a magnitude of 5 or higher. A solid circle represents a magnitude between 4.5 and 5. A plus sign represents a magnitude between about 2.3 and 4.5. Historical earthquake data are from USGS/NEIC Global Hypocenter Data Base CD-ROM (Version 3.0). Concentric circles show estimated energy centers of large prehistoric earthquakes. The estimated moment magnitude, M, for a prehistoric earthquake is located near the circle.

Note:
Epicenters of historical earthquakes are shown for the time period 1804-1992

From McNulty and Obermeier (1999)

Seismic Hazards Report for the EGC ESP Site

Epicenters of Historical Earthquakes and Estimated Energy Centers of Large Prehistoric Earthquakes in Site Region

Figure
B-1-1

s:\7900\7935\7935.000\03_0303_sect b1_fig_b1-01(02).ai (2003-05-29, 10:09)

s:\7900\7935\7935.000\03_0303_sectb1_fig_b1-02(03).ai (2003-05-29, 10:10)

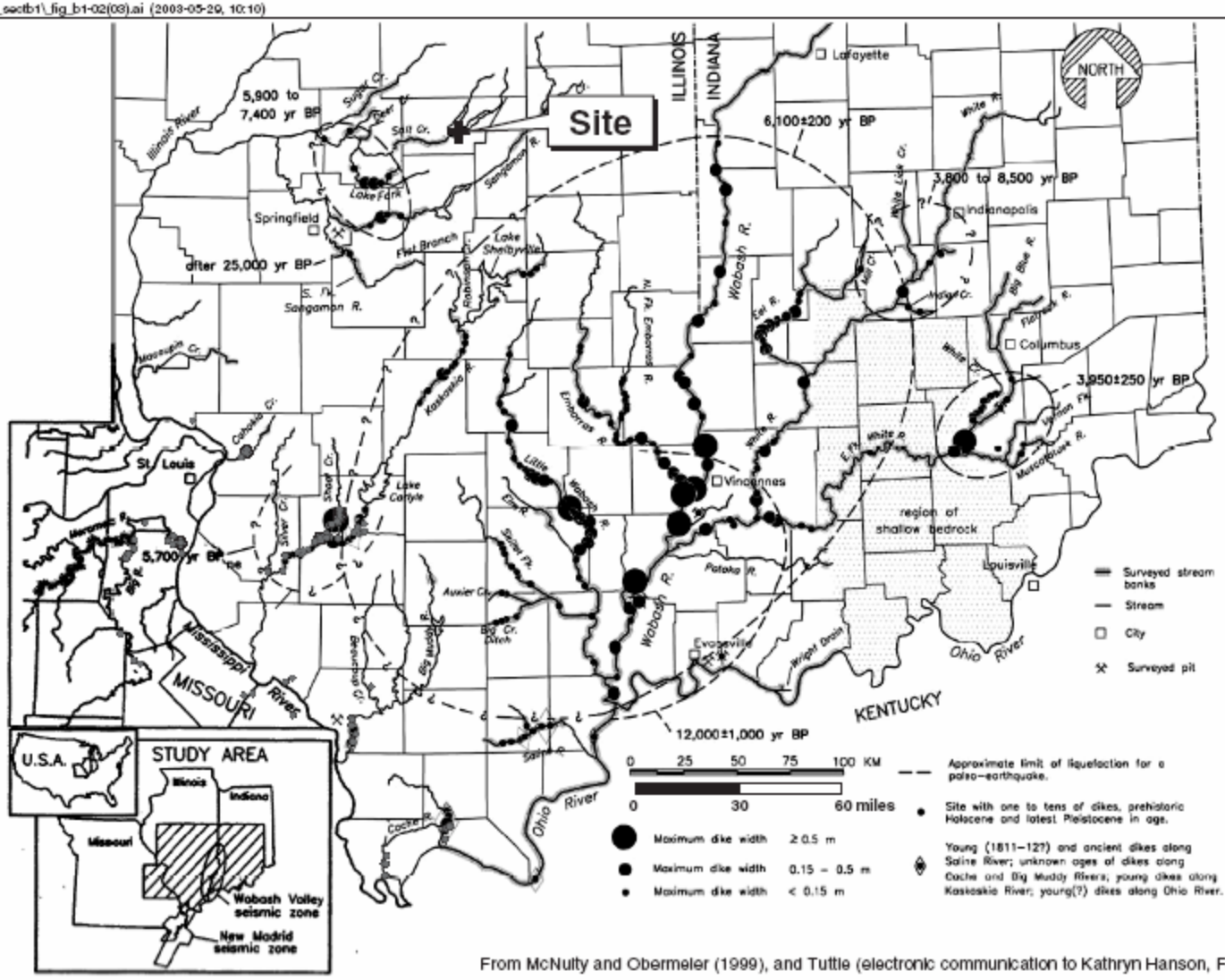

From McNulty and Obermeier (1999), and Tuttle (electronic communication to Kathryn Hanson, February 11, 2003)

Seismic Hazards Report for the EGC ESP Site

Sites of Paleoliquefaction in Southern Indiana and Illinois

Figure

B-1-2

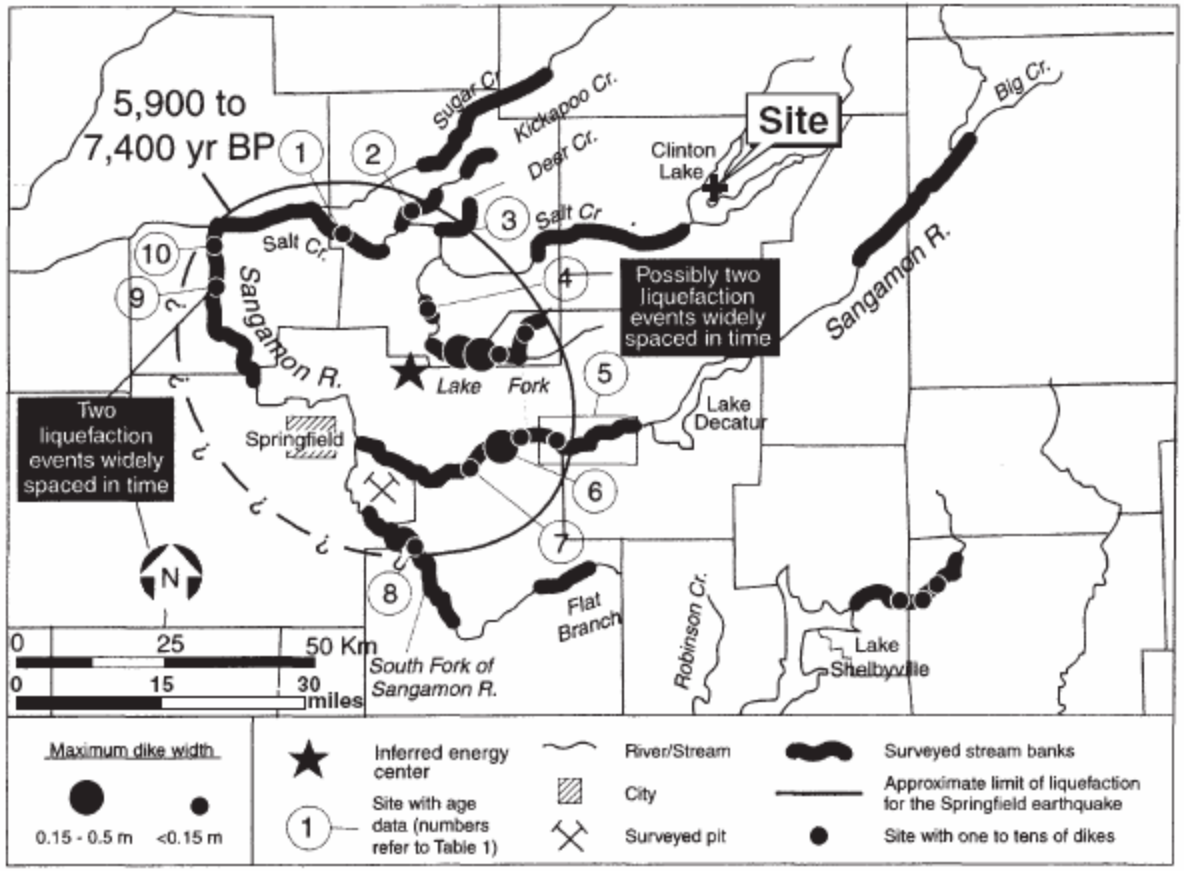

From McNulty and Obermeier (1999).

Seismic Hazards Report for the EGC ESP Site

Map of the Vicinity of the Springfield, Illinois, Earthquake Showing Approximate Limit of Liquefaction for the Earthquake

Figure
B-1-3

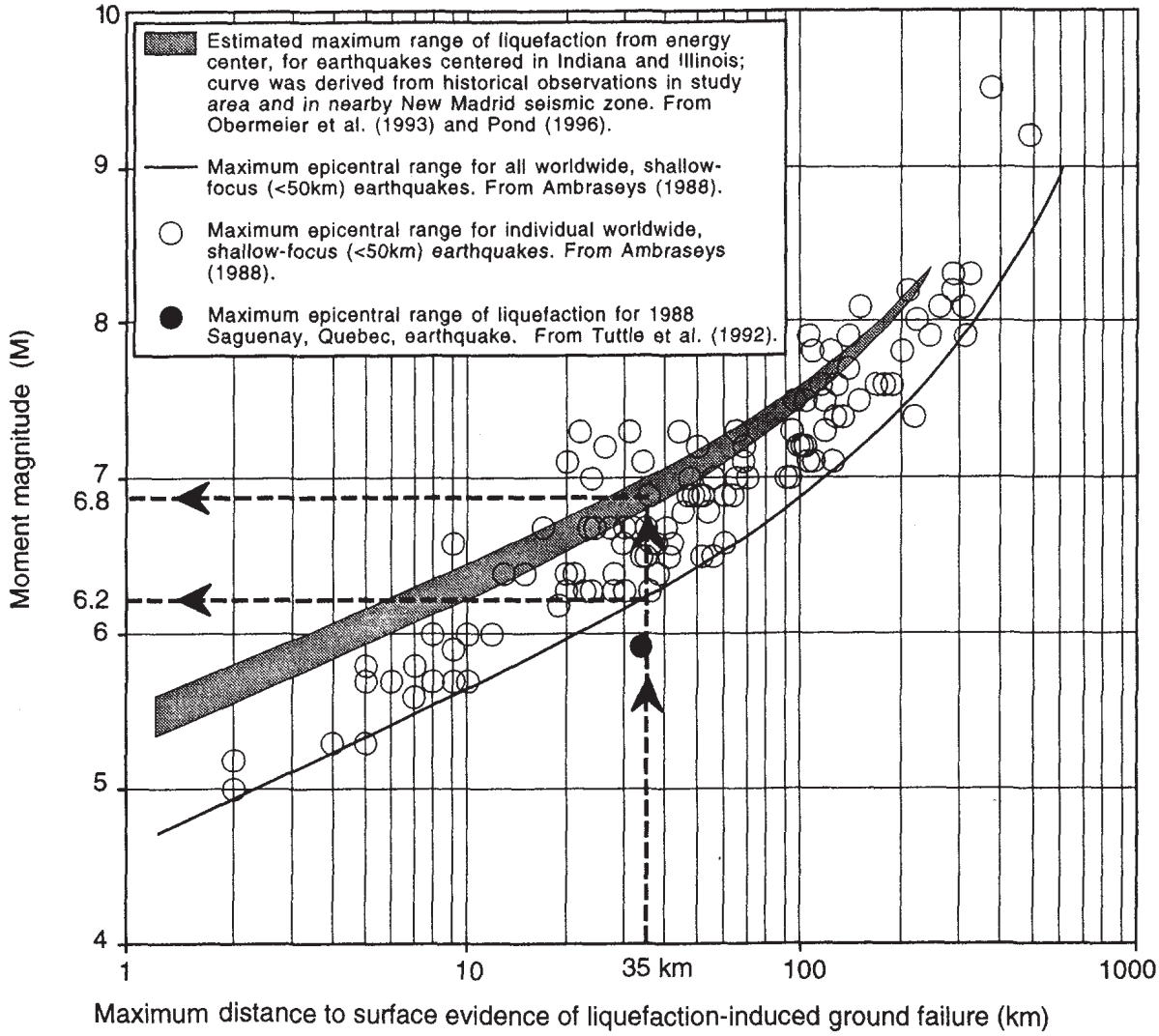

From McNulty and Obermeier (1999).

Seismic Hazards Report for the EGC ESP Site

Moment Magnitude Versus Maximum Distance to Surface Evidence of Liquefaction

Figure **B-1-4A**

S:\7900\7935\7935.000\05_1114_update_fig_b1-04a(05) [Converted].ai (11/15/2005, 09:27 am)

S:\7900\7935\7935.000\05_1114_update_fig_b1-04b.ai (11/15/2005, 09:28 am)

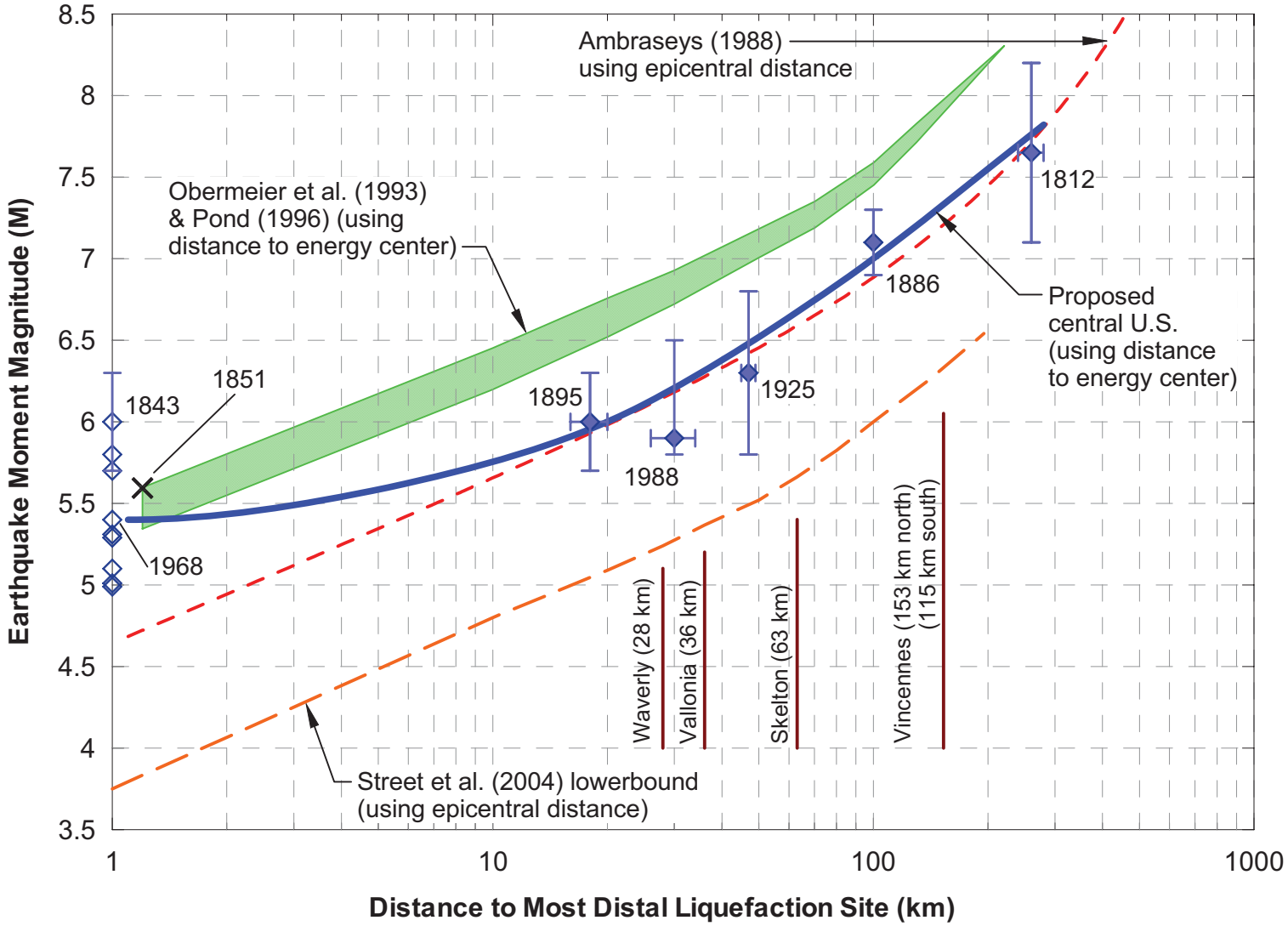

From Olson et al. (2005, in press)

Seismic Hazards Report for the EGC ESP Site

Revised Region-Specific Magnitude Bound Relation for Central United States

Figure

B-1-4B

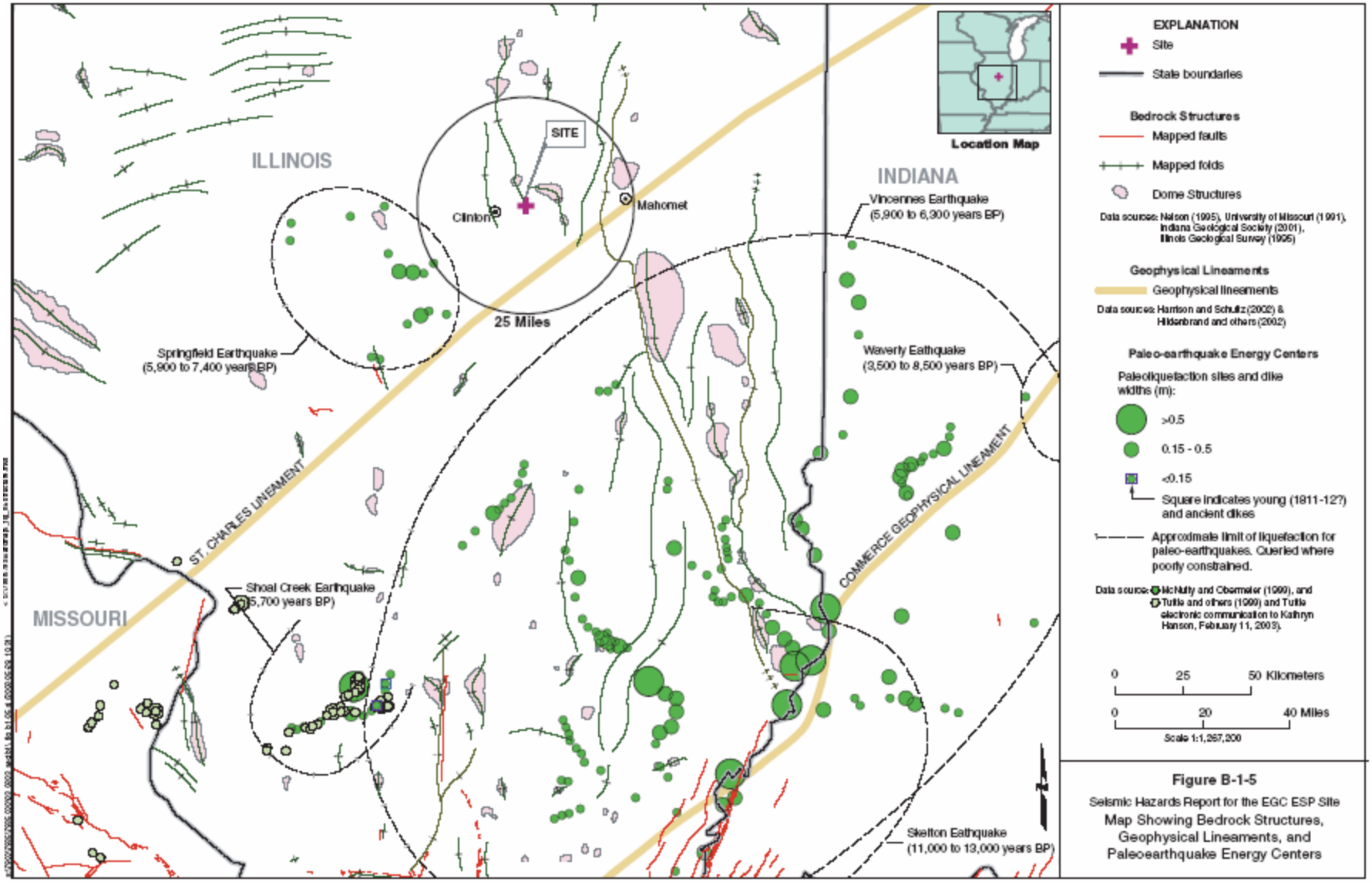

Figure B-1-5

Seismic Hazards Report for the EGC ESP Site
Map Showing Bedrock Structures, Geophysical Lineaments, and Paleoearthquake Energy Centers

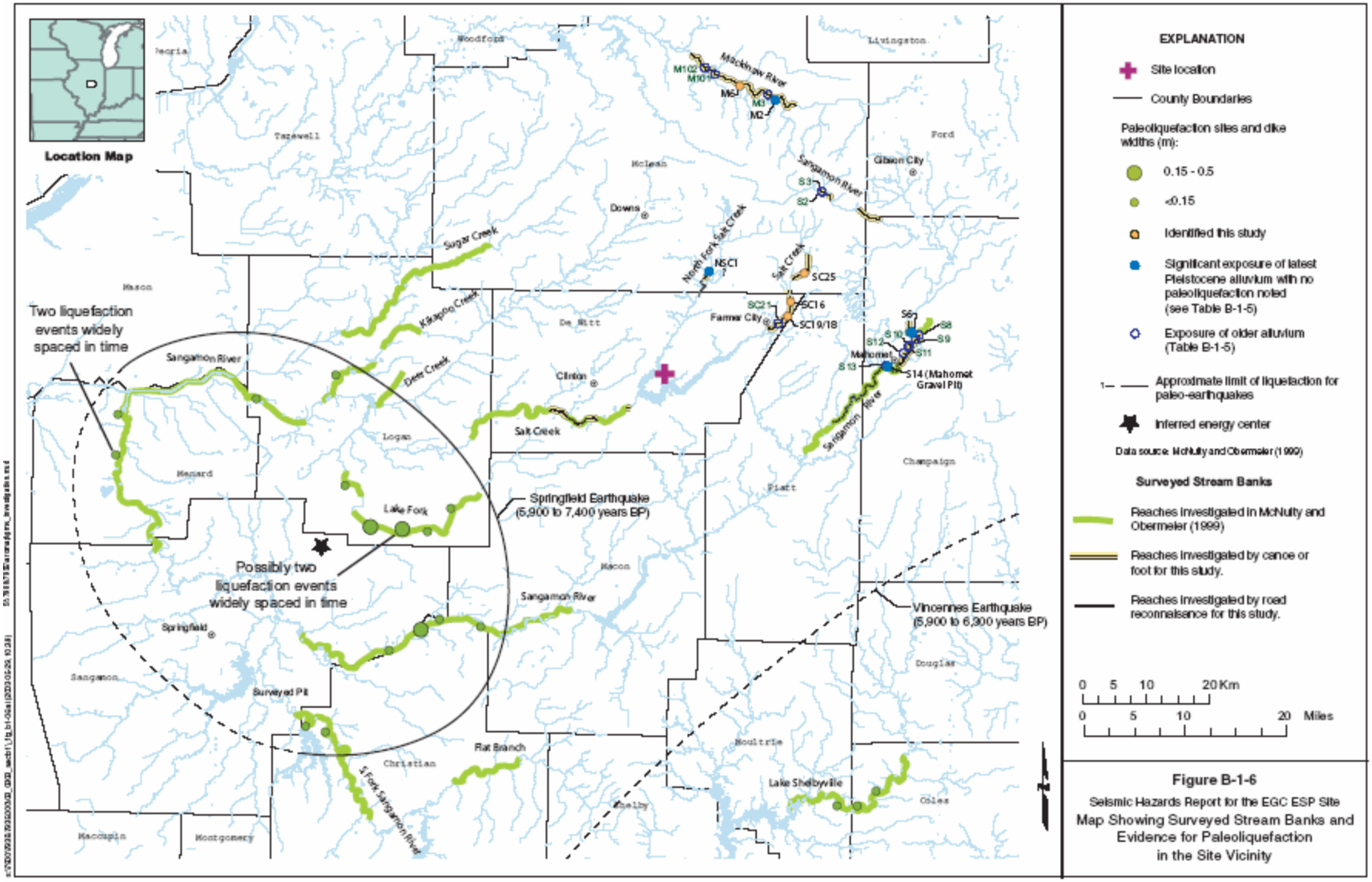

Figure B-1-6

Seismic Hazards Report for the EGC ESP Site
Map Showing Surveyed Stream Banks and Evidence for Paleoliquefaction in the Site Vicinity

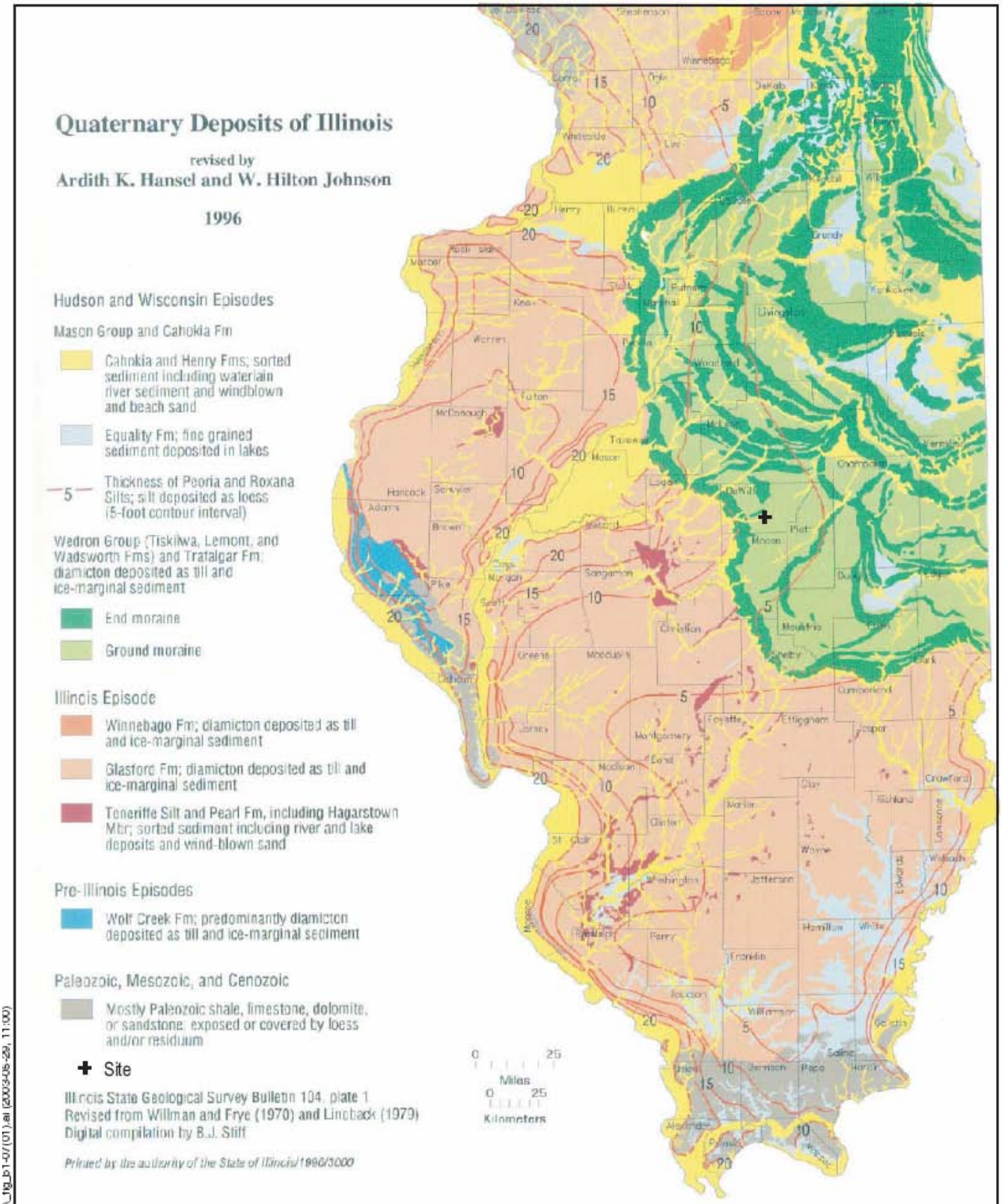

From: Hansel and Johnson (1996)

Seismic Hazards Report for the EGC ESP Site

Areal Distribution of the Wedron and Mason Groups (Wisconsin and Hudson Episodes) and Deposits of the Illinois and Pre-Illinois Episodes in Illinois

Figure
B-1-7

s:\7900\7935\7935.000703_0303_sectb1_fig_b1-07(01).ai (2003-05-29, 11:00)

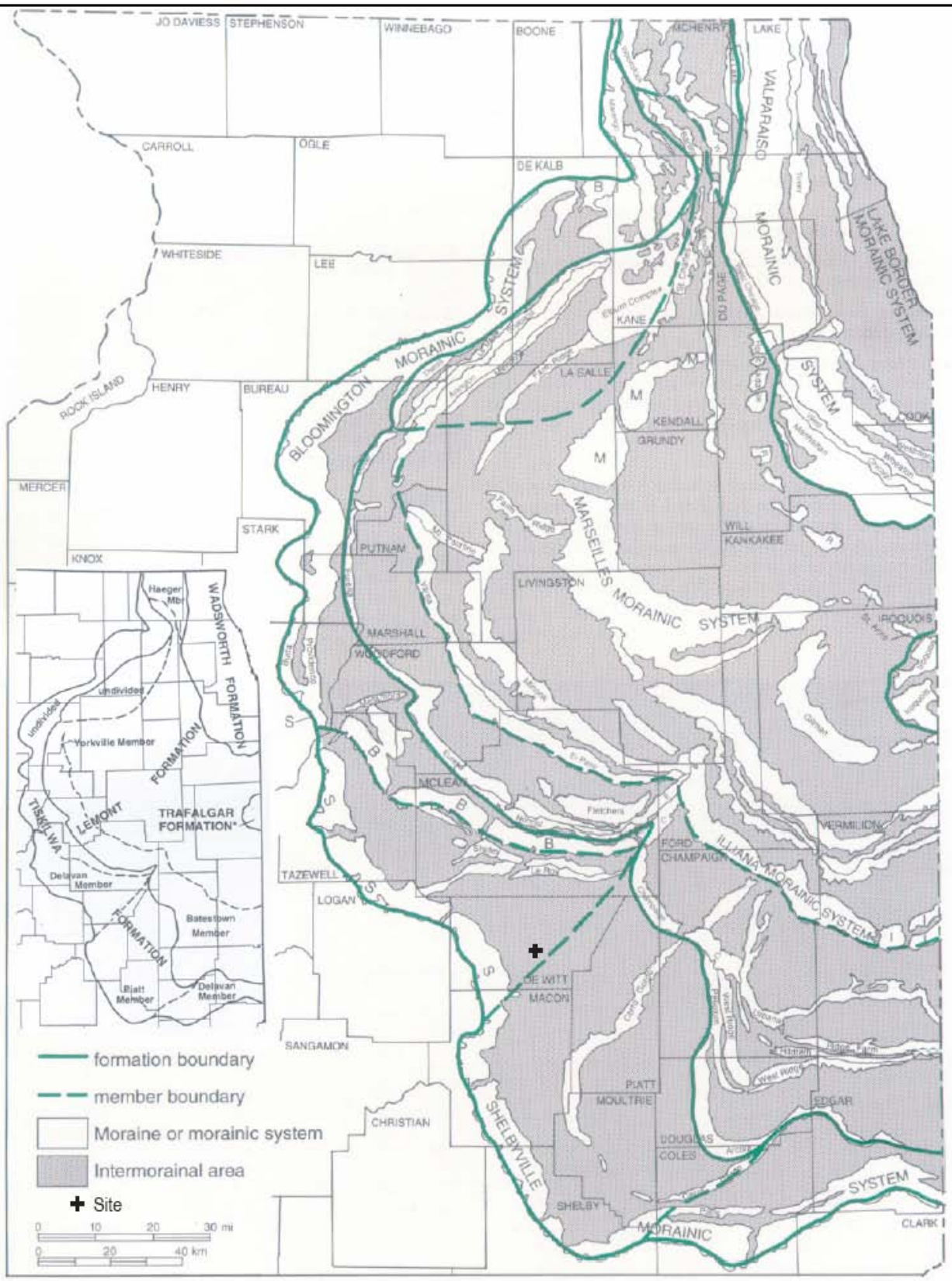

Modified from: Hansel and Johnson (1996)

Seismic Hazards Report for the EGC ESP Site
Areal distribution of moraines and boundaries of formations and principal members of the Wedron group

Figure
B-1-8

s:\79\00\793\57\935.000\03_03\03_fr_fig_a-08(15).ai (2003-05-28, 11:18)

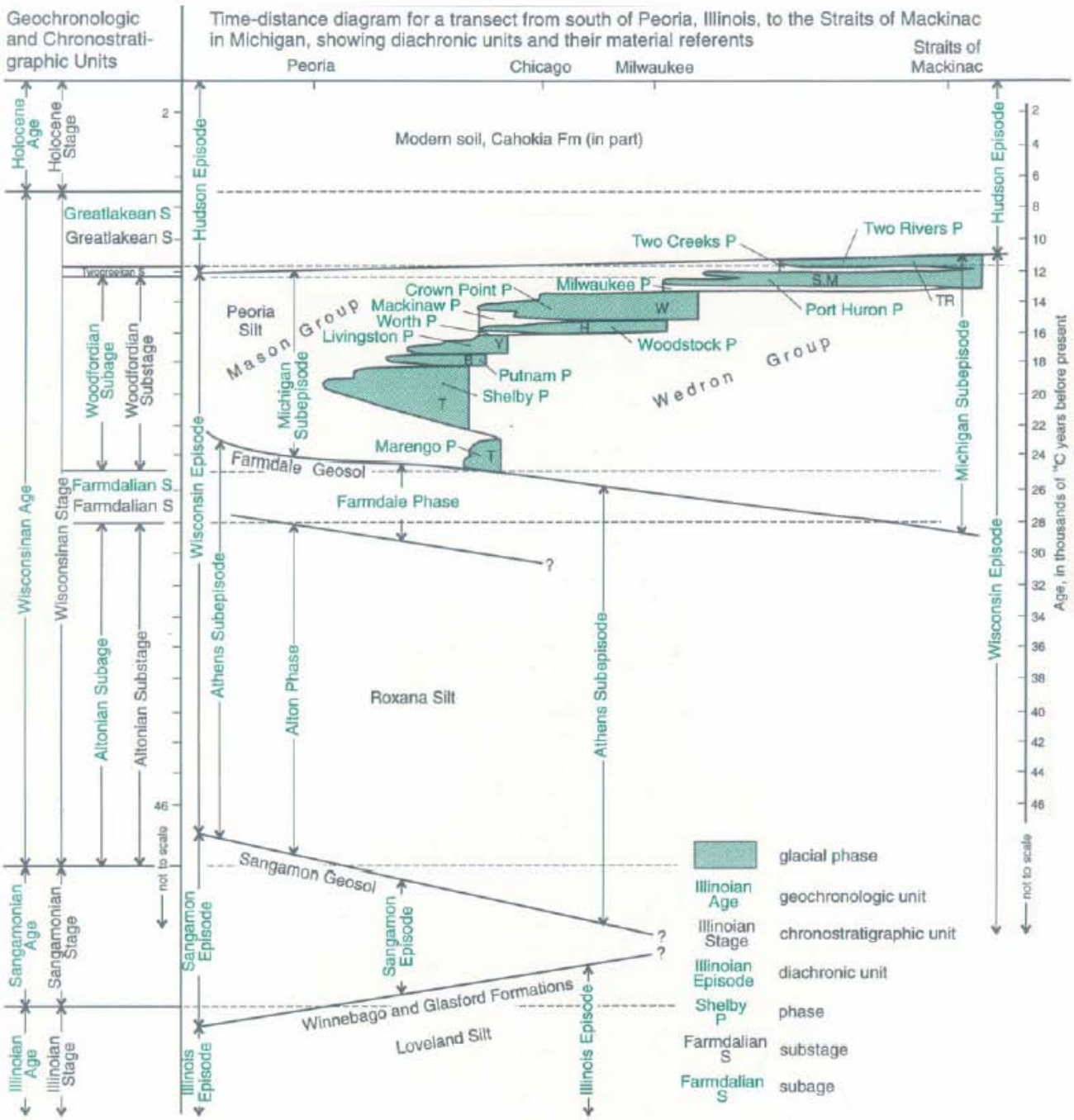

From: Hansel and Johnson (1996)

Seismic Hazards Report for the EGC ESP Site
Geochronologic Units, Chronostratigraphic Units and Diachronic Units in the Lake Michigan Lobe

Figure
B-1-9

s:\7900\7935\7935.000\03_0303_sectb1_fig_b1-09(02)_xsect.ai (2003-05-29, 11:02)

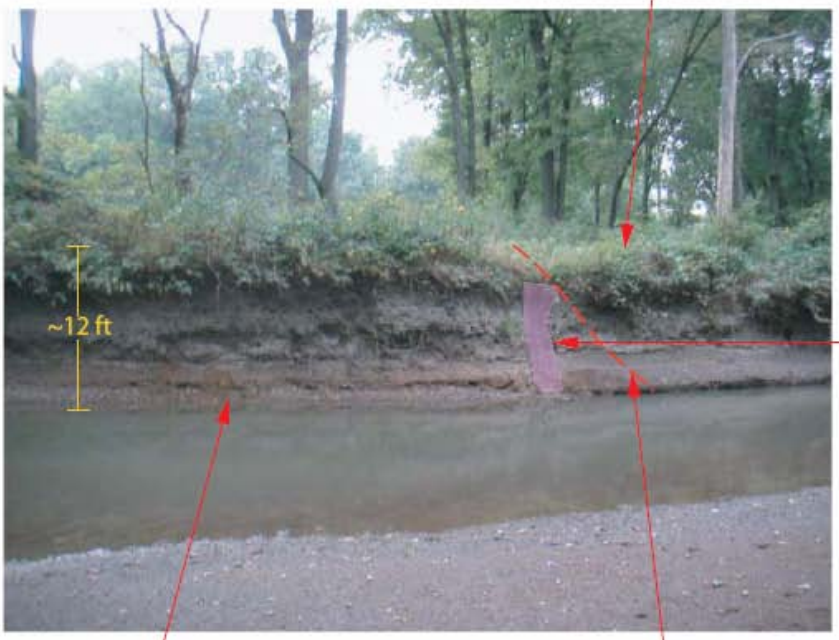

Seismic Hazards Report for the EGC ESP Site
Photograph of Riverbank Exposure on Salt Creek Showing
Fluvial Terrace Deposits of Two Ages

Figure
B-1-10

a:\79\00\793\57\935.000\03_03\03_sectb1_fig_b1-10(08).ai (2003-05-29, 11:03)

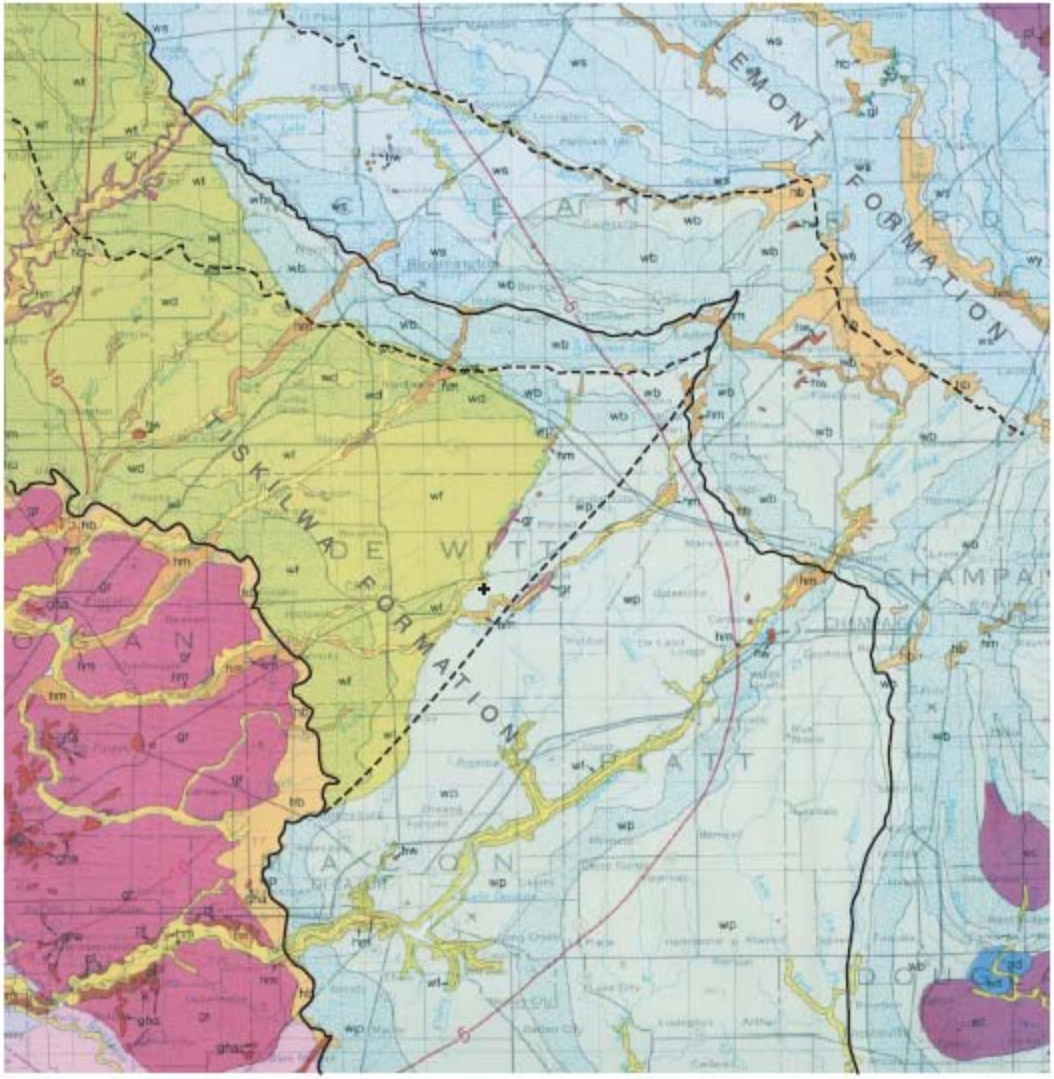

- ec — Carmi Member of Equality Formation
- ed — Dolton Member of Equality Formation
- hm — Mackinaw Member of Henry Formation
- hb — Batavia Member of Henry Formation
- hw — Wasco Member of Henry Formation

Lemont Formation:
- wy — Yorkville Till Member of Wedron Group
- ws — Snider Till Member of Wedon Group
- wb — Batestown Till Member of Wedron Group

Tiskilwa Formation:
- wp — Platt Till Member of Wedron Group
- wt — Tiskilwa Till Member of Wedron Group
- wd — Delavan Till Member of Wedron Group
- wf — Fairgrange Till Member of Wedron Group

- Moraine
- gha — Hagarstown Member of Glasford Formation
- gr — Radnor Till Member of Glasford Formation
- gv — Vandalia Till Member of Glasford Formation
- Site
- Formation boundary within the Wedron Group (from Hansel and Johnson, 1996; see Figure B-1-8)
- Member boundary within the Wedron Group (from Hansel and Johnson, 1996; see Figure B-1-8)

Notes

1. Modified from Lineback, 1979
2. More recent studies (Hansel and Johnson, 1996) reassign several members of the Wedron Group to better match moraine morphology. These new formation and member boundaries are shown here and on Figure B-1-8). Therefore, some map units on this figure may not agree with current formation and member boundaries within the Wedron Group.

0 10 20 Kilometers

0 10 20 Miles

Scale 1:500,000

Figure B-1-11

Seismic Hazards Report for the EGC ESP Site

Map Of Quaternary Deposits
In The Site Vicinity

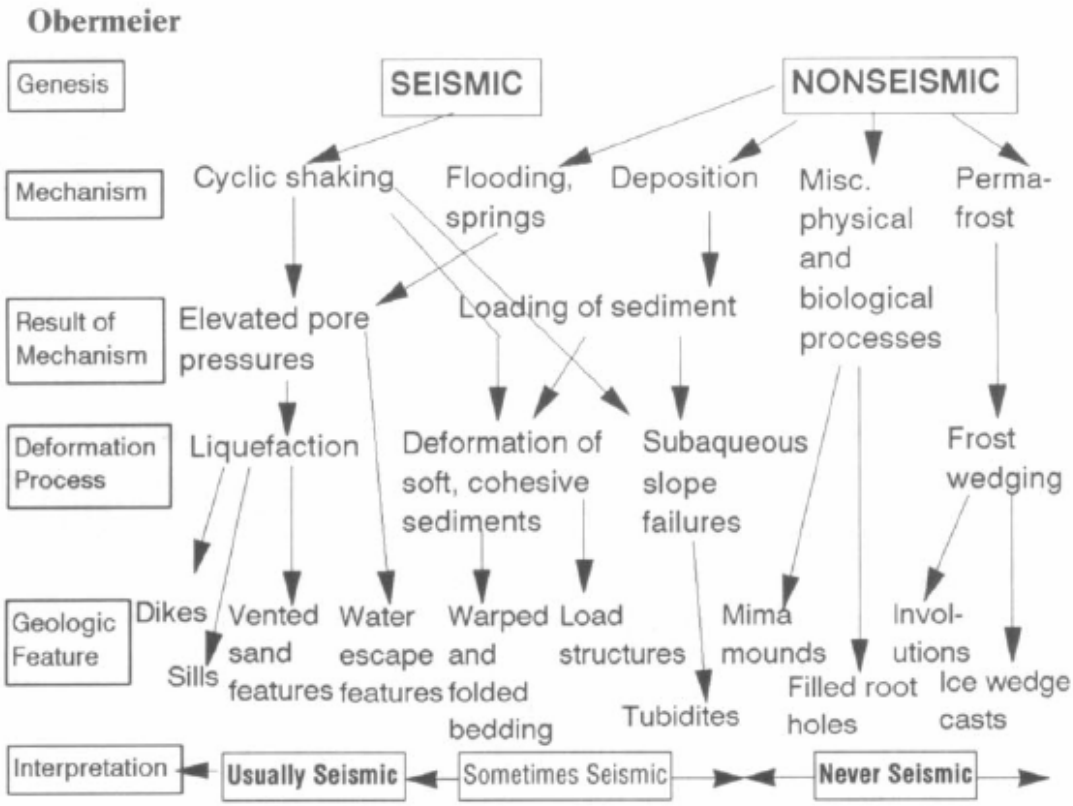

Modified from Obermeier (1996)

Seismic Hazards Report for the EGC ESP Site

Flow Chart Showing Seismic and Nonseismic Mechanisms That Create Deformation Features in Sediment

Figure B-1-12

s:\7900\7935\7935.000\03_0303_sectb1_fig_b1-12.ai (2008-05-29, 11:07)

REV1

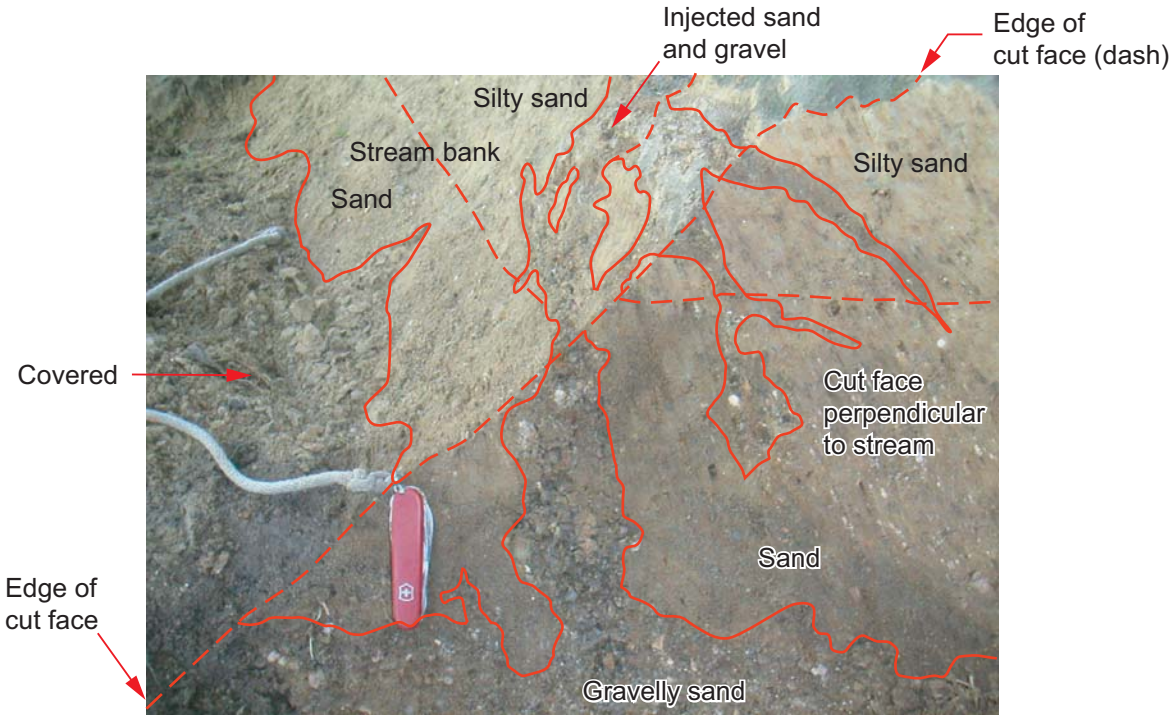

Note that:

1. Dike widens downward.
2. Gravelly sand fill fines upward.
3. Dike walls are sharp and irregular.
4. Dike is roughly tabular.
5. Dike occurs in clear association with source material.
6. Weathering within dike suggests it is relatively old.

Seismic Hazards Report for the EGC ESP Site

Photographs of Dike 1 at Locality SC 25

Figure

B-1-13A

S:\7900\7935\7935.000\03_0303_sectb1\individual_photos_0904_fig_b1-13A(09,10).ai

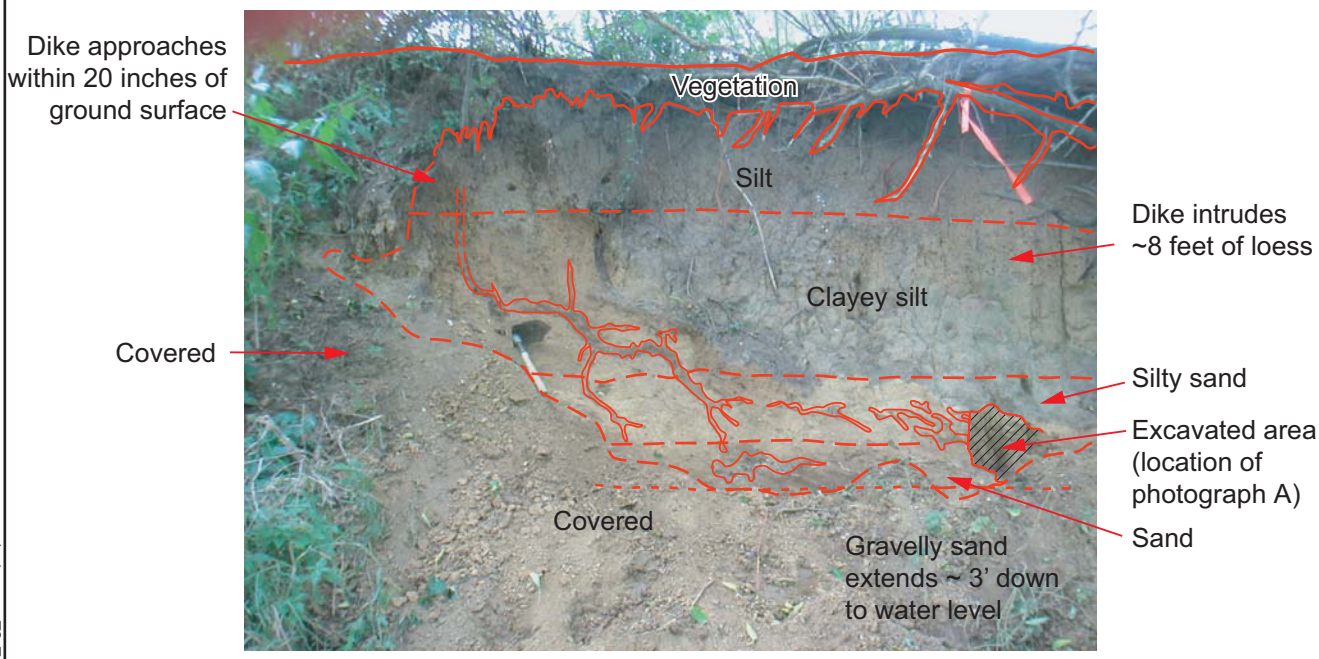

Bank rises approximately 12 feet above water level

Note that:

1. Dike widens downward.
2. Gravelly sand fill fines upward.
3. Dike walls are sharp and irregular.
4. Dike is roughly tabular.
5. Dike occurs in clear association with source material.
6. Weathering within dike suggests it is relatively old.

Seismic Hazards Report for the EGC ESP Site

Photographs of Dike 1 at Locality SC 25

Figure

B-1-13B

S:\7900\7935\7935.000\03_0303_sectb1\individual_photos_0904_fig_b1-13B(10).ai

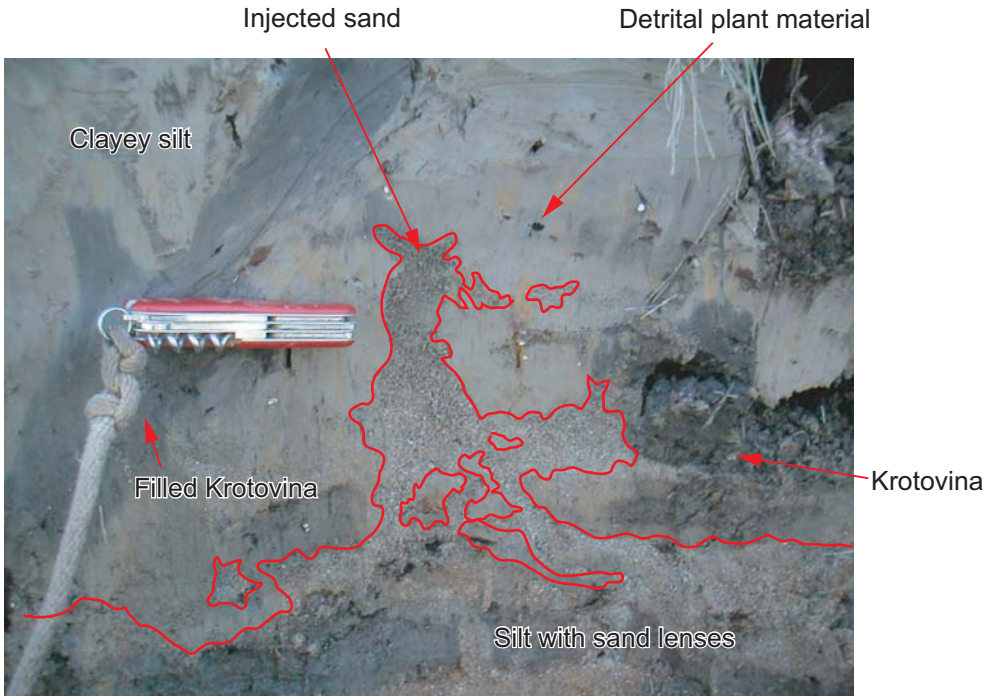

Note that:

1. Dike widens downward.
2. Sand in filling fines upwards.
3. Contacts are sharp and irregular.
4. Dike occurs in clear association with source material.
5. Dike includes clasts of silty clay, apparently ripped from its walls.
6. Maximum dike width is 1.5 in.

Seismic Hazards Report for the EGC ESP Site

Photograph of Dike 2 at Locality SC 19

Figure

B-1-14

s:\7900\7935\7935.000\03_0303_sectb1_fig_b1-14(07)_0904.ai

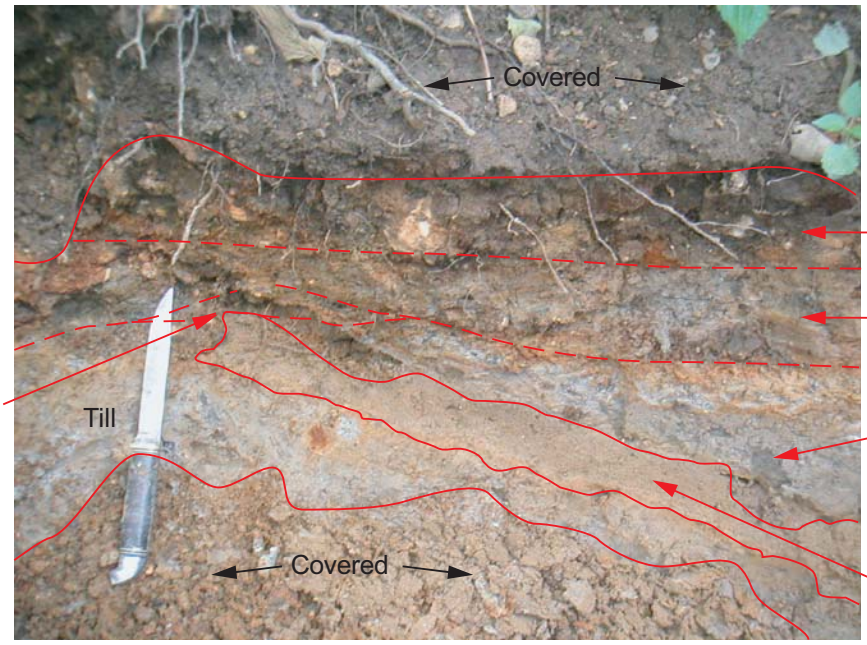

Note: Knife is 8 in. long

Seismic Hazards Report for the EGC ESP Site

Photographs of Parts of Dike 1 at Locality M 6

Figure

B-1-15A

s:\7900\7935\7935.000\03_0303_sectb1\individual_photos_0904_fig_B1-15A(13).ai

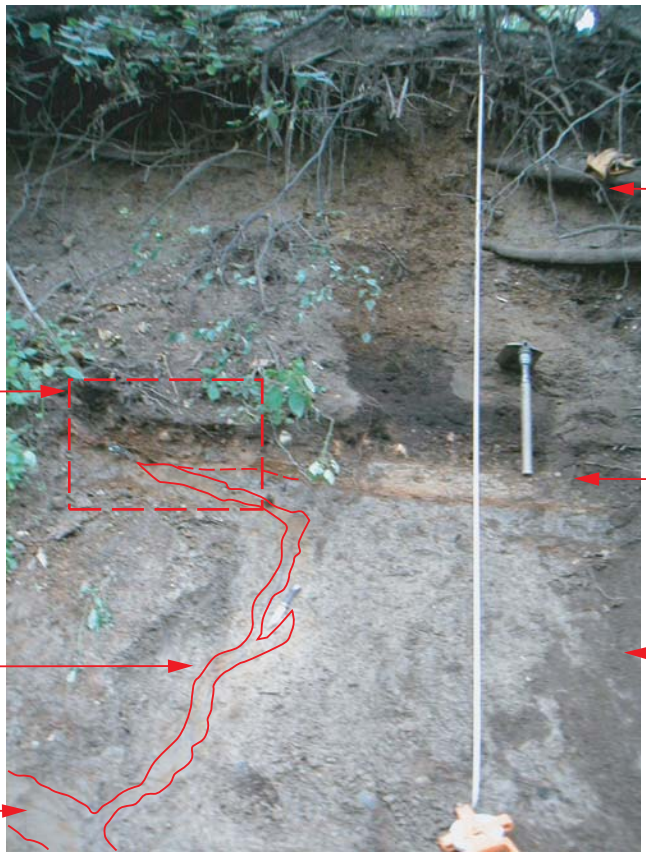

Seismic Hazards Report for the EGC ESP Site

Photographs of Parts of Dike 1 at Locality M 6

Figure

B-1-15B

s:\7900\7935\7935.000\03_0303_sectb1\individual_photos_0904_fig_B1-15B(12).ai

Seismic Hazards Report for the EGC ESP Site

Photograph of Thick Silt Layer Overlaying Fluvial Deposit at Locality S14

Figure
B-1-16

s:\79/00\79/35.00/03_00/3_sect01_fig_b1-16(14).ai (2003-05-29, 11:14)

Exhibit 1 to Attachment 1
to the Seismic Hazards Report
for the Exelon Generation Company, LLC
Early Site Permit
Site Safety Analysis Report
Appendix B

EXHIBIT 1

Radiocarbon Dating

BETA

Consistent Accuracy Delivered On Time.

Beta Analytic Inc.
4985 SW 74 Court
Miami, Florida 33155 USA
Tel: 305 667 5167
Fax: 305 663 0964
beta@radiocarbon.com
www.radiocarbon.com

MR. DARDEN HOO
Directo

Mr. Ronald Hatfiel
Mr. Christopher Patric
Deputy Directo

December 6, 2002

Mr. Hans Abramson
Geomatrix Consultants, Incorporated
2101 Webster Street, 12th Floor
Oakland, CA 94612
USA

RE: Radiocarbon Dating Results For Samples 7935_SC-19-2.1, 7935_SC-19-2.2

Dear Mr. Abramson:

Enclosed are the radiocarbon dating results for two samples recently sent to us. They each provided plenty of carbon for accurate measurements and all the analyses went normally. The report sheet also contains the method used, material type, applied pretreatments and, where applicable, the two sigma calendar calibration range.

As always, this report has been both mailed and sent electronically. All results (excluding some inappropriate material types) which are less than about 20,000 years BP and more than about ~250 BP include this calendar calibration page (also digitally available in Windows metafile (wmf) format upon request). The calibrations are calculated using the newest (1998) calibration database with references quoted on the bottom of each page. Multiple probability ranges may appear in some cases, due to short term variations in the atmospheric 14C contents at certain time periods. Examining the calibration graphs will help you understand this phenomenon. Don't hesitate to contact us if you have questions about calibration.

We analyzed these samples on a sole priority basis. No students or intern researchers who would necessarily be distracted with other obligations and priorities were used in the analyses. We analyzed them with the combined attention of our entire professional staff.

Information pages are also enclosed with the mailed copy of this report. If you have any specific questions about the analyses, please do not hesitate to contact us.

Our invoice is enclosed. Please, forward it to the appropriate officer or send VISA change authorization. Thank you. As always, if you have any questions or would like to discuss the results, don't hesitate to contact me.

Sincerely,

Darden Hood

BETA

BETA ANALYTIC INC.

DR. M.A. TAMERS and MR. D.G. HOOD

UNIVERSITY BRANCH
4985 S.W. 74 COURT
MIAMI, FLORIDA, USA 33155
PH: 305/667-5167 FAX: 305/663-0964
E-MAIL: beta@radiocarbon.com

REPORT OF RADIOCARBON DATING ANALYSES

Mr. Hans Abramson

Report Date: 12/6/02

Geomatrix Consultants, Incorporated

Material Received: 10/25/02

Sample Data	Measured Radiocarbon Age	13C/12C Ratio	Conventional Radiocarbon Age(*)
Beta - 171950 SAMPLE : 7935_SC-19-2.1 ANALYSIS : AMS-Standard delivery MATERIAL/PRETREATMENT : (plant material): acid/alkali/acid 2 SIGMA CALIBRATION : Cal BC 9150 to 8750 (Cal BP 11100 to 10700)	9620 +/- 40 BP	-29.4 o/oo	9550 +/- 40 BP
Beta - 171951 SAMPLE : 7935_SC-19-2.2 ANALYSIS : AMS-Standard delivery MATERIAL/PRETREATMENT : (plant material): acid/alkali/acid 2 SIGMA CALIBRATION : Cal BC 10390 to 9780 (Cal BP 12340 to 11730)	10260 +/- 40 BP	-26.6 o/oo	10230 +/- 40 BP

Dates are reported as RCYBP (radiocarbon years before present, "present" = 1950A.D.). By International convention, the modern reference standard was 95% of the C14 content of the National Bureau of Standards' Oxalic Acid & calculated using the Libby C14 half life (5568 years). Quoted errors represent 1 standard deviation statistics (68% probability) & are based on combined measurements of the sample, background, and modern reference standards.

Measured C13/C12 ratios were calculated relative to the PDB-1 international standard and the RCYBP ages were normalized to -25 per mil. If the ratio and age are accompanied by an (*), then the C13/C12 value was estimated, based on values typical of the material type. The quoted results are NOT calibrated to calendar years. Calibration to calendar years should be calculated using the Conventional C14 age.

CALIBRATION OF RADIOCARBON AGE TO CALENDAR YEARS

(Variables: C13/C12=-29.4:lab. mult=1)

Laboratory number:	**Beta-171950**
Conventional radiocarbon age:	**9550±40 BP**
2 Sigma calibrated result: (95% probability)	**Cal BC 9150 to 8750 (Cal BP 11100 to 10700)**

Intercept data

Intercepts of radiocarbon age with calibration curve:	Cal BC 9100 (Cal BP 11050) and Cal BC 9020 (Cal BP 10970) and Cal BC 8810 (Cal BP 10760)
1 Sigma calibrated results: (68% probability)	Cal BC 9120 to 8990 (Cal BP 11070 to 10940) and Cal BC 8910 to 8780 (Cal BP 10860 to 10730)

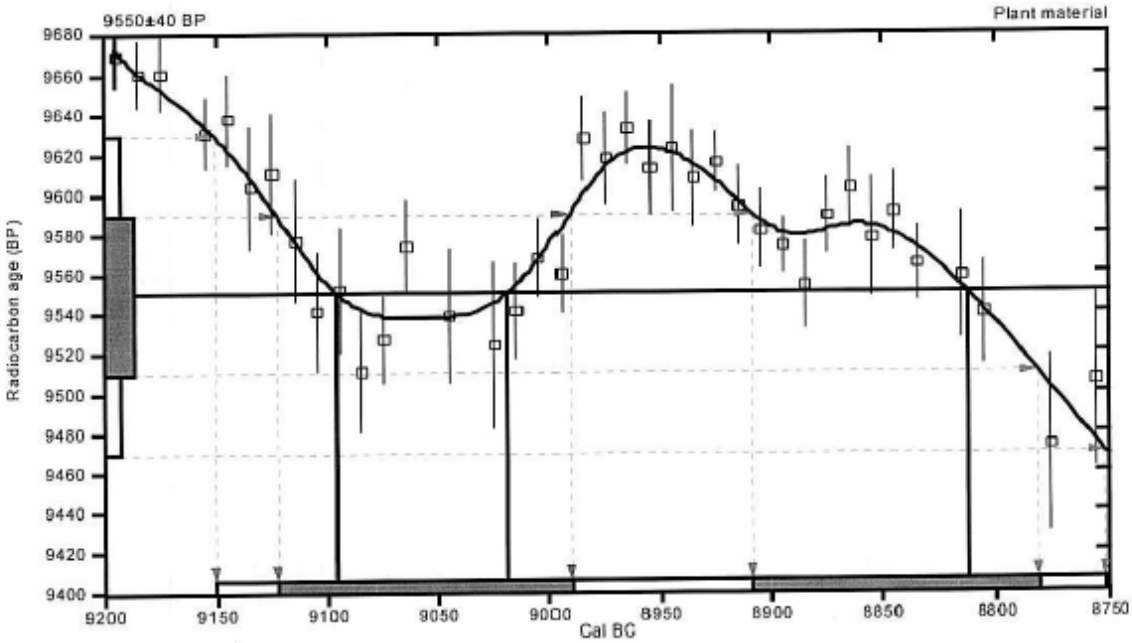

References:

Database used

Calibration Database
Editorial Comment
Stuiver, M., van der Plicht, H., 1998, Radiocarbon 40(3), pxii-xiii
INTCAL98 Radiocarbon Age Calibration
Stuiver, M., et. al., 1998, Radiocarbon 40(3), p1041-1083
Mathematics
A Simplified Approach to Calibrating C14 Dates
Talma, A. S., Vogel, J. C., 1993, Radiocarbon 35(2), p317-322

Beta Analytic Inc.

4985 SW 74 Court, Miami, Florida 33155 USA • Tel: (305) 667 5167 • Fax: (305) 663 0964 • E-Mail: beta@radiocarbon.com

CALIBRATION OF RADIOCARBON AGE TO CALENDAR YEARS

(Variables: C13/C12=-26.6:lab. mult=1)

Laboratory number:	**Beta-171951**
Conventional radiocarbon age:	**10230±40 BP**
2 Sigma calibrated result: (95% probability)	**Cal BC 10390 to 9780 (Cal BP 12340 to 11730)**

Intercept data

Intercept of radiocarbon age with calibration curve:	Cal BC 10000 (Cal BP 11950)
1 Sigma calibrated result: (68% probability)	Cal BC 10360 to 9860 (Cal BP 12310 to 11810)

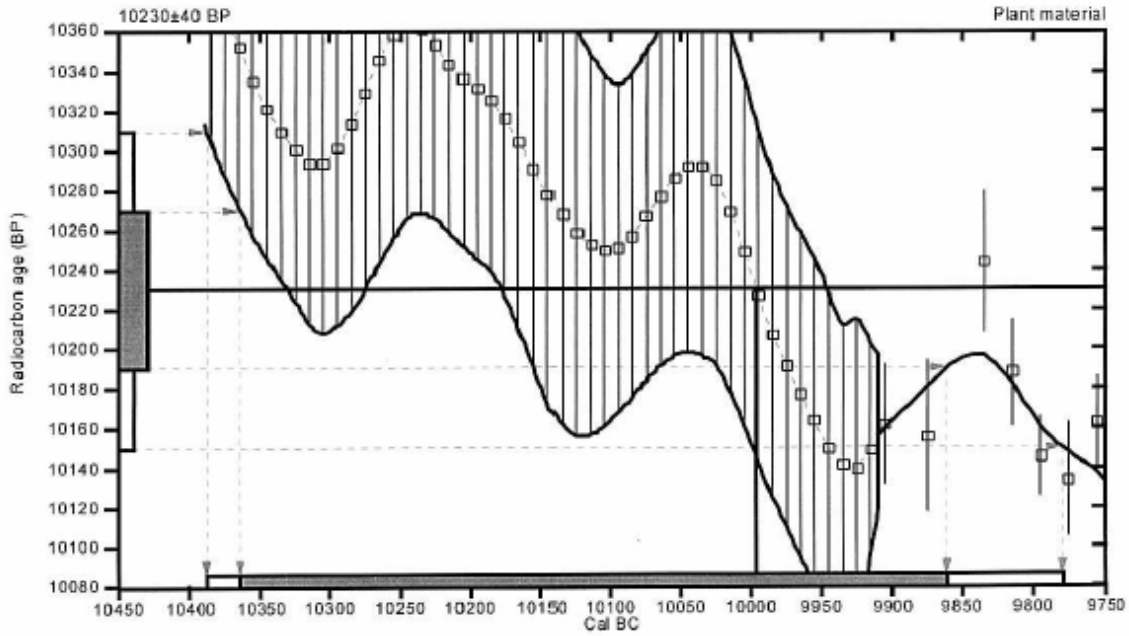

References:

Database used

Calibration Database
Editorial Comment
Stuiver, M., van der Plicht, H., 1998, Radiocarbon 40(3), pxii-xiii
INTCAL98 Radiocarbon Age Calibration
Stuiver, M., et. al., 1998, Radiocarbon 40(3), p1041-1083
Mathematics
A Simplified Approach to Calibrating C14 Dates
Talma, A. S., Vogel, J. C., 1993, Radiocarbon 35(2), p317-322

Beta Analytic Inc.

4985 SW 74 Court, Miami, Florida 33155 USA • Tel: (305) 667 5167 • Fax: (305) 663 0964 • E-Mail: beta@radiocarbon.com

BETA

Consistent Accuracy Delivered On Time.

Beta Analytic Inc.
4985 SW 74 Court
Miami, Florida 33155 USA
Tel: 305 667 5167
Fax: 305 663 0964
beta@radiocarbon.com
www.radiocarbon.com

MR. DARDEN HOOD
Director

Mr. Ronald Hatfield
Mr. Christopher Patrick
Deputy Directors

December 12, 2002

Mr. Hans Abramson
Geomatrix Consultants, Incorporated
2101 Webster Street, 12th Floor
Oakland, CA 94612
USA

RE: Radiocarbon Dating Result For Sample 7935_S-6-2

Dear Mr. Abramson:

Enclosed is the radiocarbon dating result for one sample recently sent to us. It provided plenty of carbon for an accurate measurement and the analysis went normally. As usual, the method of analysis is listed on the report sheet and calibration data is provided where applicable.

As you may remember we discussed the sample material, as we were not sure of the actual origin given the lack of normal wood grain or striations. I contacted you to express my concerns as to if the material might be coal or some other geologic material. SEM analysis performed prior to the dating indicated that the material did indeed appear to be charcoal, although possessing little actual structure. Per your instructions we proceeded with the dating. As you see the age is quite a bit older than expected and this probably indicates re-depositing or re-use of material from a previous time.

As always, no students or intern researchers who would necessarily be distracted with other obligations and priorities were used in the analysis. It was analyzed with the combined attention of our entire professional staff.

If you have specific questions about the analyses, please contact us. We are always available to answer your questions.

The cost of analysis was previously invoiced. As always, if you have any questions or would like to discuss the results, don't hesitate to contact me.

Sincerely,

Darden Hood

BETA

BETA ANALYTIC INC.

DR. M.A. TAMERS and MR. D.G. HOOD

UNIVERSITY BRANCH
4985 S.W. 74 COURT
MIAMI, FLORIDA, USA 33155
PH: 305/667-5167 FAX: 305/663-0964
E-MAIL: beta@radiocarbon.com

REPORT OF RADIOCARBON DATING ANALYSES

Mr. Hans Abramson

Report Date: 12/12/02

Geomatrix Consultants, Incorporated

Material Received: 10/25/02

Sample Data	Measured Radiocarbon Age	13C/12C Ratio	Conventional Radiocarbon Age(*)
Beta - 171952 SAMPLE : 7935_S-6-2 ANALYSIS : AMS-Standard delivery MATERIAL/PRETREATMENT : (charred material): acid/alkali/acid	35510 +/- 1200 BP	-25.4 o/oo	35500 +/- 1200 BP

Dates are reported as RCYBP (radiocarbon years before present, "present" = 1950A.D.). By International convention, the modern reference standard was 95% of the C14 content of the National Bureau of Standards' Oxalic Acid & calculated using the Libby C14 half life (5568 years). Quoted errors represent 1 standard deviation statistics (68% probability) & are based on combined measurements of the sample, background, and modern reference standards.

Measured C13/C12 ratios were calculated relative to the PDB-1 international standard and the RCYBP ages were normalized to -25 per mil. If the ratio and age are accompanied by an (*), then the C13/C12 value was estimated, based on values typical of the material type. The quoted results are NOT calibrated to calendar years. Calibration to calendar years should be calculated using the Conventional C14 age.

Attachment 2 to the Seismic Hazards Report for the Exelon Generation Company, LLC Early Site Permit

Site Safety Analysis Report Appendix B

Contents

1. Recurrence for New Madrid Characteristic Earthquakes ...……..……. **B2-1-1**
1.1 Estimation of the Time Interval between Prehistoric New Madrid Earthquakes….……...…….……. B2-1-1
2.1 Estimation of Recurrence Model paramers ..……..……...…….… B2-1-2
2.1.1 Time-Independent (Poisson) Recurrence …….. B2-1-3
2.1.2 Time Dependent Recurrence ……... B2-1-4
2. References ……..……..……..…….. B2-2-1

Tables

B-2-1 Age Constraints Used for Assessment of Recurrence of New Madrid Characteristic Earthquakes.....B2.T-1
B-2-2 Discrete Distributions for Rate of Characteristic New Madrid Earthquakes..... B2.T-3

Figures

B-2-1 Illustration of Simulation Process for Evaluating Time Intervals Between Characteristic New Madrid Earthquakes
B-2-2 Mean Repeat Time for New Madrid Characteristic Earthquakes

CHAPTER 1

Recurrence for New Madrid Characteristic Earthquakes

This attachment to Appendix B of the Site Safety Analysis Report (SSAR) for the Exelon Generating Company (EGC) Early Site Permit (ESP) Site presents an assessment of the recurrence of characteristic earthquakes on the central faults of the New Madrid seismic zone (NMSZ). Section 2.1.5.2.1 of Appendix B describes the paleoliquefaction investigations that have been conducted in the NMSZ region. These investigations have identified a number of paleoliquefaction features interpreted to have been caused by earthquakes and that have provided estimated age dates for these features. Table 2.1-5 of Appendix B summarizes the age dates for samples taken from these features, including the 95-percent confidence interval on the corrected calendar year for each sample. Various assessments of the paleoliquefaction features have interpreted them to be due to recurrence of characteristic earthquakes on the central faults of the NMSZ. The characteristic earthquake interpretation has been used for the EGC ESP analysis discussed in this Attachment. The first step in the recurrence assessment is to use these age dates and their uncertainties to provide constraints on the dates for prehistoric earthquakes. The intervals between these estimated dates then provide a sample of the repeat times between assumed characteristic earthquakes on the central New Madrid faults. The second step is to use these repeat times to estimate the parameters of appropriate recurrence models for the earthquakes. For this assessment, the uncertainties in the estimated dates were propagated through the estimation process using Monte Carlo simulation.

1.1 Estimation of the Time Interval between Prehistoric New Madrid Earthquakes

The process used to estimate the time interval between prehistoric New Madrid liquefaction events is illustrated on Figure B-2-1. Part (a) shows an example data set of dates and their 95-percent confidence intervals for samples taken from individual paleoliquefaction features. The various symbols indicate whether the feature is identified to have formed before or after event 'Y' (the earthquake of ~ AD 1450) or event 'X' (the earthquake of ~ AD 900). The first step was to simulate a set of possible dates for each sample using the defined uncertainty limits. A normal distribution for the sample date was for the date estimation error assumed, and the 95-pecent confidence interval was used to define the $\pm 2\sigma$ range for the age. Part (b) of Figure B-2-1 shows such a simulation using the data set from part (a).

The possible set of dates for individual samples in part (b) can now be used to constrain the possible ages for the prehistoric earthquakes. The oldest post-liquefaction date and the youngest pre-liquefaction date define the range of possible dates for each paleoearthquake. For example, the solid circles shown in part (b) of Figure B-2-1 indicate samples taken from features that postdate event Y. The oldest of these is considered to provide an estimate of

the youngest date for event Y. The solid squares shown in part (b) of Figure B-2-1 indicate samples taken from features that predate event Y and the youngest of these provides an estimate of the oldest date for event Y. These two sample dates thus provide a date range for event Y, shown by dashed lines. A similar assessment provides an estimated data range for event X.

The actual dates for the individual events were then simulated from these date ranges. The true date was assumed to be uniformly distributed within the possible date range. The uniform distribution represents the maximum uncertainty distribution for a parameter when all that is known is the range of possible values. Part (c) of Figure B-2-1 shows an example simulation result for the dates of the prehistoric earthquakes. The simulated dates for the prehistoric events, along with the 1811 to 1812 earthquake sequence date, define a sample of the time interval between characteristic earthquakes that can be used to estimate the parameters of a recurrence model. This estimation can include the open interval from 1811-1812 to the present.

The uncertainty in estimated time intervals between prehistoric earthquakes was captured through Monte Carlo simulation. One hundred sets of sample ages (part b of Figure B-2-1) were simulated. For each set of simulated sample ages, 100 simulations of prehistoric earthquake dates were created. The resulting 10,000 samples of time intervals between characteristic earthquakes were then used to develop 10,000 estimates of recurrence parameters as described in Section 1.2 of this attachment. Separate simulations were performed using data from the northeastern, central and southwestern portions of the NMSZ. The individual samples used in the analysis are given in Table B-2-1. The statistics of the simulated ages for the prehistoric earthquakes are summarized in the following table. The ages obtained for the three data sets are similar.

Statistics of Estimated Dates for Prehistoric NMSZ Characteristic Earthquakes

Event	Event Date		
	Northeast Data Set	Central Data Set	Southwest Data Set
Y	1453 AD ±56 years	1421 AD ±18 years	1448 AD ±17 years
X	890 AD ±31 years	917 AD ±29 years	922 AD ±35 years

1.2 Estimation of Recurrence Model Parameters

Two general types of recurrence models have been used to characterize the occurrence of characteristic earthquakes, time-independent and time-dependent. The time independent or

Poisson model is the recurrence model commonly use in probabilistic seismic hazard analysis (PSHA) formulations for earthquakes of all sizes and was the recurrence model used in the Electric Power Research Institute Seismic Owner Group (EPRI-SOG) characterization of earthquake recurrence for all sources. The implication of this model is that the time interval between events is exponentially distributed (with the mode at zero), and a coefficient of variation of the time intervals is equal to 1.0. The likelihood of occurrence of an earthquake in any time interval is independent of when the previous event occurred. However, the physics of the process of stress accumulation followed by release in characteristic earthquake ruptures on faults has led a number of investigators to consider time-dependent recurrence models for these sources. In the simplest form, time-dependent recurrence models are cast as a renewal model in which the likelihood of the next characteristic event occurring in a specified time interval is dependent only on the elapsed time since the previous characteristic event (e.g., Cornell and Winterstein, 1988; Wu et al., 1995). These models typically use a skewed distribution, such as the lognormal, Weibull, or gamma, to represent the distribution of times between characteristic earthquakes. Recently the Working Group on California Earthquake Probabilities (Working Group, 2003) has used these types of models to characterize the likelihood of large earthquakes on faults in the San Francisco Bay area. Cramer (2001) used a lognormal distribution to estimate the average repeat time for large earthquake in the NMSZ based on the estimated earthquake dates presented in Tuttle and Schweig (2000). In the following, recurrence model parameters are estimated for characteristic New Madrid earthquakes using both time independent and time-dependent recurrence models.

1.2.1 Time-Independent (Poisson) Recurrence

For the time-independent or Poisson recurrence model, the time interval between earthquakes, t, is exponential distributed with probability density given by:

$$f(t) = \lambda e^{-\lambda t} \qquad \text{(Eq. B-2-1)}$$

and cumulative probability given by

$$F(t) = 1 - e^{-\lambda t} \qquad \text{(Eq. B-2-2)}$$

where λ is the average rate of characteristic events ($1/\lambda$ is the average time between events).

Given a sample of n time intervals and one open interval, t_0, the likelihood function for the observed data set is given by:

$$L(\lambda) = \left\{ \prod_{i=1}^{n} f(t_i) \right\} \{1 - F(t_0)\} \qquad \text{(Eq. B-2-3)}$$

The maximum likelihood solution for the mean rate is given by the expression:

$$\lambda_{\text{maximum likelihood}} = \frac{n}{\sum_{i=1}^{n} t_i + t_0} \qquad \text{(Eq. B-2-4)}$$

An empirical uncertainty distribution for the parameter λ can be determined by computing the likelihood of observing the sample of event inter-arrival times (t_i ..t_n and t_0) for a range

values of λ, and then normalizing these likelihoods to form a discrete probability distribution. This process was used to develop a probability distribution for λ for each set of simulated prehistoric earthquake dates. The resulting 10,000 likelihood distributions were then averaged to produce a composite uncertainty distribution for λ. The top plot of Figure B-2-2 shows the resulting cumulative distributions for the average time between events, $1/\lambda$, estimated from the three sets of simulation of times for events X, Y, and the open interval post 1811-1812. The three data sets (northeast, central, and southwest) produce very similar distributions for mean repeat time. Therefore, the simulations from all three data sets were used to develop a composite distribution, shown in the bottom plot of Figure B-2-2. This distribution was represented in the hazard analysis by a five-point discrete approximation to a continuous distribution defined by Miller and Rice (1983). This discrete distribution is listed in Table B-2-2.

1.2.2 Time-Dependent Recurrence

For the time-dependent renewal recurrence model, there are a variety of distributions that have been used to model the variability in the time between events, such as the lognornmal, Weibull, and gamma distributions. Recently, Matthews et al. (2002) have proposed a model based on the inverse Gaussian distribution for inter-arrival times of repeated large ruptures on a fault. This model, termed the Brownian Passage Time (BPT) model was used by the Working Group (2003) to assess the probabilities of large earthquakes in the San Francisco Bay area. Ellsworth et al. (1999) and Matthews et al. (2002) propose that the BPT model is more representative of the physical process of strain buildup and release on a seismic source than the other distribution forms that have been used for renewal models (e.g., the lognormal). Based on these arguments, the BPT model was used in this analysis.

For the BPT model, the time interval between earthquakes, t, is distributed with probability density given by:

$$f(t) = \left(\frac{\mu_{In}}{2\pi\alpha^2 t^3} \right)^{1/2} \exp\left(-\frac{(t-\mu_{In})^2}{2\mu_{In}\alpha^2 t} \right) \qquad \text{(Eq. B-2-5)}$$

and cumulative probability given by

$$F(t) = \Phi[u_1(t)] + e^{2/\alpha^2}\Phi[-u_2(t)]$$

$$u_1(t) = \left(\sqrt{t/\mu_{In}} - \sqrt{\mu_{In}/t}\right)/\alpha \qquad \text{(Eq. B-2-6)}$$

$$u_2(t) = \left(\sqrt{t/\mu_{Int}} + \sqrt{\mu_{In}t/t}\right)/\alpha$$

where $\mu_{\ln t}$ is the mean inter-arrival time (repeat time), α is the aperiodicity coefficient (coefficient of variation of t), and $\Phi(\,)$ is the standard normal cumulative probability function.

Given a sample of n time intervals and one open interval, t_0, the likelihood function for the observed data set is again given by equation (B-2-3) with $f(t)$ and $F(t)$ replaced by equations (B-2-5) and (B-2-6). The maximum likelihood solution must be found by numerical

methods. Because of the very limited data set, the estimate of the aperiodicity coefficient, α, is highly uncertain. Therefore, the value of α was constrained to values reported from examination of larger data sets. Based on examination of a number of data sets, the Working Group (2003) developed an uncertainty distribution for the aperiodicity coefficient for the BTP model consisting of three weighted values of 0.3 (0.2), 0.5 (0.5), and 0.7 (0.3). The Working Group (2003) weighted distribution was adopted to constrain the value of α.

The process described in Section 1.2.1 of this Attachment was repeated to develop an empirical distribution for $\mu_{\ln t}$, given a specified value of α using the combined simulations for the dates of events X and Y using the northeastern, central, and southern sites. For each simulated set of dates for the prehistoric New Madrid earthquakes, equations (B-2-3), (B-2-5), and (B-2-6) were used to compute the likelihood of observing the sample for a range of values of $\mu_{\ln t}$. These likelihoods were normalized to define a discrete distribution for $\mu_{\ln t}$. The estimation process was repeated for each of the 10,000 simulated sets of dates and the resulting distributions averaged to produce a composite distribution for $\mu_{\ln t}$. These distributions are shown in the lower plot on Figure B-2-2. These distributions were represented in the hazard analysis by the five-point discrete approximations to a continuous distribution listed in Table B-2-2.

For the renewal recurrence model, the probability of an earthquake in the next time interval Δt is given be the expression:

$$P_{renewal}(\text{event in time } t_0 \text{ to } t_0 + \Delta t) = \frac{F(t_0 + \Delta t) - F(t_0)}{1 - F(t_0)} \qquad \text{(Eq. B-2-7)}$$

The basic PSHA formulation used to assess the site hazard assumes that the occurrence of individual earthquakes conforms to a Poisson process. In order to combine the hazard from earthquakes defined by a renewal process into the total hazard, an equivalent Poisson rate is defined such that a Poisson process will given a probability of at least one earthquake in time interval Δt is that is equal to the probability given by equation (B-2-7). The equivalent Poisson rate, $\lambda_{renewal}$, is given by the expression:

$$\lambda_{renewal} = -\ln\left[1 - P_{renewal}(\text{event in time } t_0 \text{ to } t_0 + \Delta t)\right] / \Delta t \qquad \text{(Eq. B-2-8)}$$

A time period of 60 years was chosen as the time period of interest for the ESP application (20-year application period plus 40-year plant design life). The time t was set at October 1, 2005. The corresponding estimates of $\lambda_{renewal}$ are listed in Table B-2-2.

The last column of Table B-2-2 lists the average equivalent repeat time for characteristic earthquakes derived from the discrete distributions for λ or $\lambda_{renewal}$. The values in bold are the inverse of the weighted average event frequency for each model. Assigning equal weight to the Poisson and renewal models, the resulting weighted average frequency of characteristic events is 1/465 events per year.

CHAPTER 2

References

Cornell, C.A., and S.R. Winterstein. "Temporal and Magnitude Dependence in Earthquake Recurrence Models." *Bulletin of the Seismological Society of America*. Vol. 78, No. 4. pp. 1522-1537. 1988.

Cramer, C.H. "A Seismic Hazard Uncertainty Analysis for the New Madrid Seismic Zone." *Engineering Geology*. Vol. 62. pp. 251-266. 2001.

Ellsworth, W.L., M.V. Matthews, R.M. Nadeau, S.P. Nishenko, P.A. Reasenberg, and R.W. Simpson. "A Physically-based Earthquake Recurrence Model for Estimation of Long-Term Earthquake Probabilities." *Proceedings of the Workshop on Earthquake Recurrence: State of the Art and Directions for the Future*. Istituto Nazionale de Geofisica. Rome, Italy. February 22-25. 1999.

Kelson, K.I., R.B. Van Arsdale, G.D. Simpson, and W.R. Lettis. "Assessment of the Style and Timing of Surficial Deformation along the Central Reelfoot Scarp, Lake County, Tennessee." *Seismological Research Letters*. Vol. 63, No. 3. pp. 349-356. 1992.

Kelson, K.I., G.D. Simpson, R.B. Van Arsdale, C.C. Haraden, and W.R. Lettis. "Multiple Late Holocene Earthquakes along the Reelfoot Fault, Central New Madrid Seismic Zone." *Journal of Geophysical Research*. Vol. 101, No. B3. pp. 6151-6170. 1996.

Li, Y., E.S. Schweig, M.P. Tuttle, and M.A. Ellis. "Evidence for Large Prehistoric Earthquakes in the Northern New Madrid Seismic Zone, Central United States." *Seismological Research Letters*. Vol. 69. pp. 270-276. 1998.

Matthews, M.V., W.L. Ellsworth, and P.A. Reasenberg. "A Brownian Model for Recurrent Earthquakes." *Bulletin of the Seismological Society of America*. Vol. 92. No. 6. pp. 2233-2250. 2002.

Miller, A.C., and T.R. Rice. Discrete Approximations of Probability Distributions." *Management Science*. Vol. 29, No. 3, pp. 352-362. 1983.

Tuttle, M.P. *Late Holocene Earthquakes and their Implications for Earthquake Potential of the New Madrid Seismic Zone, Central United States*. Ph.D. Dissertation. University of Maryland. 250 pp. 1999.

Tuttle, M.P. "The Use of Liquefaction Features in Paleoseismology: Lessons Learned in the New Madrid Seismic Zone, Central United States." *Journal of Seismology*. Vol. 5. pp. 361-380. 2001.

Tuttle, Martitia P. M. Tuttle & Associates. Written (Electronic) Communication. February 27, 2003.

Tuttle, M.P., and E.S. Schweig. "The Earthquake Potential of the New Madrid Seismic Zone." *American Geophysical Union, EOS Transactions*. Vol. 81, No. 19, p. S308. 2000.

Tuttle, M.P., and E.S. Schweig. *Towards a Paleoearthquake Chronology for the New Madrid Seismic Zone*. Collaborative Research, M. Tuttle & Associates and Eastern Region Hazards Team, U.S. Geological Survey. Annual Report Submitted to the U.S. Geological Survey. USGS External Project No. 1434-99HQGR0022. 18 pp. 2001.

Tuttle, M.P., and L.W. Wolf. *Towards a Paleoearthquake Chronology for the New Madrid Seismic Zone.* Progress Report Submitted to the U.S. Geological Survey NEHRP. USGS External Project No. 1434-01HQGR0164. 36 pp. 2003.

Tuttle, M.P., J.D. Sims, K. Dyer-Williams, R.H. Lafferty III, and E.S. Schweig III. *Dating of Liquefaction Features in the New Madrid Seismic Zone.* U. S. Nuclear Regulatory Commission Report NUREG/GR-0018. 42 pp. (plus appendices). 2000.

Working Group on California Earthquake Probabilities (Working Group). "Earthquake Probabilities in the San Francisco Bay Region: 2002-2031." U.S. Geological Survey Open-File Report 03-214. 2003.

Wu, S.-C., CA. Cornell, and S.R. Winterstein. "A Hybrid Recurrence Model and Its Implication on Seismic Hazard Results." *Bulletin of the Seismological Society of America*. Vol. 85, No. 1. pp. 1-16. 1995.

TABLE B-2-1

AGE CONSTRAINTS USED FOR ASSESSMENT OF RECURRENCE OF NEW MADRID CHARACTERISTIC EARTHQUAKES
Seismic Hazards Report for the ECG ESP Site

Name of Site	Lab Sample Number[1]	Material	Time Relationship of Sample to Event	Age (95% Probability Interval)
Amanda Northeast Set	Beta-133006 (T2-C14)	Charcoal (top of lower sand blow)	Pos Y	AD 1520 to 1690
	Beta-133005 (T2-C13)	Charcoal (19 cm below sand blow)	Pre Y	AD 1020 to 1210
		Artifacts, including diagnostic ceramics	Pre Y	AD 800 to 1400
Bugg Central Set	Beta-108883	Charcoal	Post X	AD 167 to 1950
Central Ditch 1 Southwest Set	Beta-108869	Charcoal	Post X	AD 1690 to 1740
	Beta-81308	Soil (30 cm thick, with few small artifacts possibly reworked)	Post X	AD 1000 to 1240
	Beta-81309	Soil; artifacts	Pre X	AD 790 to 1020
Current River 2 Southwest Set	Beta-110225	Charcoal	Post Y	AD 1300 to 1450
	Beta-110223	Cypress knees	Pre Y	AD 1310 to 1480
	Beta-110224	Charcoal	Pre Y	AD 1240 to 1440
Dillahunty Central Set	Beta-166248 (C5)	Charcoal from base of soil developed in sand-blow crater	Post Y	AD 1400 to 1490
	Beta-171218 (FSN4)	Maize kernel fragment from 0 to 10 cm below sand blow	Pre Y	AD 910 to 1210
Dodd Central Se	Beta-142449	Charred corn kernel from aboriginal wall trench dug into sand blow	Post Y	AD 1410 to 1460
	Beta-119102	Charcoal	Pre Y	AD 1290 to 1410
	Beta-102502	Charcoal	Pre Y	AD 1220 to 1300

TABLE B-2-1

AGE CONSTRAINTS USED FOR ASSESSMENT OF RECURRENCE OF NEW MADRID CHARACTERISTIC EARTHQUAKES
Seismic Hazards Report for the ECG ESP Site

Name of Site	Lab Sample Number[1]	Material	Time Relationship of Sample to Event	Age (95% Probability Interval)
Eaker 1 Southwest Set	Beta-91511	Charcoal (vertical root)	Post Y	AD 1690 to 1740
	Beta-75326	Charcoal	Post Y	AD 1650 to 1950
	Beta-81313	Soil; ceramics	Pre Y	AD 1180 to 1400
Eaker 2 Southwest Set	NA	Ceramics	Post X	AD 800 to 1000
	Beta-86810	Charcoal	Post X	AD 1400 to 1630
	Beta-86811	Charcoal	Post X	AD 1310 to 1480
	Beta-77450	Charcoal	Post X	AD 1270 to 1420
	Beta-86190	Soil	Post X	AD 1180 to 1310
	Beta-86816	Soil and ceramics	Pre X	AD 470 to 780
Eaker 3 Southwest Set	Beta-69618	Charcoal and artifacts	Post X	AD 1460 to 1800
	NA	Ceramics	Pre X	AD 800 to 1000
Haynes Central Set	G-19080	Charcoal	Post X	AD 1300 to 1660
Hillhouse Northeast Set	Beta-102500	Charcoal and ceramics	Post X	AD 780 to 1000
	Beta-102499	Charcoal	Pre X	AD 790 to 1010
Johnson 5 Northeast Set	Beta-102505	Soil	Pre X	AD 770 to 1040
K1 Champey Pocket Northeast Set	Beta-49608	Charcoal	Post Y	AD 1430 to 1650
	Beta-49609	Charcoal	Pre Y	AD 1220 to 1390
	Beta-48553	Charcoal; artifacts	Post X	AD 430 to 890
K2 Proctor City Northeast Set	CAMS-13559	Charcoal	Pre Y	AD 1260 to 1410
	CAMS-13540	Charcoal	Post X	AD 980 to 1220
	CAMS-13537	Charcoal	Pre X	AD 780 to 1030
Kochtitzky Ditch 1	Beta-97574 Artifacts	Charcoal	Pre Y	AD 990 to 1220

TABLE B-2-1

AGE CONSTRAINTS USED FOR ASSESSMENT OF RECURRENCE OF NEW MADRID CHARACTERISTIC EARTHQUAKES
Seismic Hazards Report for the ECG ESP Site

Name of Site	Lab Sample Number[1]	Material	Time Relationship of Sample to Event	Age (95% Probability Interval)
Southwest Set	Beta-102512	Charcoal	Post Y	AD 1440 to 1660
L2 Northeast Set	Beta-71234	Soil (dispersed carbon)	Post X	AD 770 to 1040
New Franklin 3 Central Set	Beta-97577	Soil	Post X	AD 890 to 1170
	Beta-97578	Soil	Post X	AD 860 to 1020
	Beta-86191	Soil	Post X	AD 690 to 990
Central Set	Beta-97578	Soil	Post X	AD 860 to 1020
	Beta-86191	Soil	Post X	AD 690 to 990
Obion 200 Northeast Set	Beta-146738	Wood W2 collected from silt deposit above sand blow	Post Y	AD 1530 to 1680
	Beta-146737	Wood W1 collected within 1 cm of base of sand blow	Pre Y	AD 1300 to 1420
Obion 216 Northeast Set	Beta-152008	Wood (W2 from outer 1 cm of horizontally bedded log buried by sand blow)	Pre Y	AD 1060 to 1080 AD 1150 to 1290
	Beta-152009	Wood (W4 from outer 1 cm of tree trunk in growth position in clay deposit beneath sand blow.	Pre Y	AD 1160 to 1300
Walker Southwest Set	Beta-133018 (T2-C2)	Charcoal from cultural horizon < 1 cm below sand blow; artifacts	Pre Y	AD 1420 to 1500
Yarbro 3 Central Set	Beta-84977	Tree	Post Y	AD 1680 to 1760
	Beta-108882	Tree center	Pre Y	AD 1445 to 1670 Plus 68 rings (AD 1513 to 1738)

TABLE B-2-2

DISCRETE DISTRIBUTIONS FOR RATE OF CHARACTERISTIC NEW MADRID EARTHQUAKES

Seismic Hazards Report for the ECG ESP Site

Recurrence Model	$1/\lambda$ (events/year)	$\exp(\mu_{lnt})$ (years)	Event Frequency λ or $\lambda_{renewal}$ (events/year)	Weight	Equivalent Average Repeat Time (years)
Poisson	161		6.20E-03	0.10108	161
	262		3.82E-03	0.24429	262
	410		2.44E-03	0.30926	410
	694		1.44E-03	0.24429	694
	1,563		6.40E-04	0.10108	1,563
					366
Renewal (Lognormal $\sigma_{lnt} = 0.3$)		333	3.39E-03	0.10108	295
		410	1.07E-03	0.24429	935
		485	3.02E-04	0.30926	3,311
		574	5.95E-05	0.24429	16,807
		709	4.30E-06	0.10108	232,558
					1,404
Renewal (Lognormal $\sigma_{lnt} = 0.5$)		316	4.85E-03	0.10108	206
		440	2.18E-03	0.24429	459
		573	8.89E-04	0.30926	1,125
		746	2.58E-04	0.24429	3,876
		1,032	2.97E-05	0.10108	33,670
					733
Renewal (Lognormal $\sigma_{lnt} = 0.7$)		325	4.45E-03	0.10108	225
		506	2.25E-03	0.24429	444
		719	1.02E-03	0.30926	980
		1,011	3.37E-04	0.24429	2,967
		1,521	4.49E-05	0.10108	22,272
					713

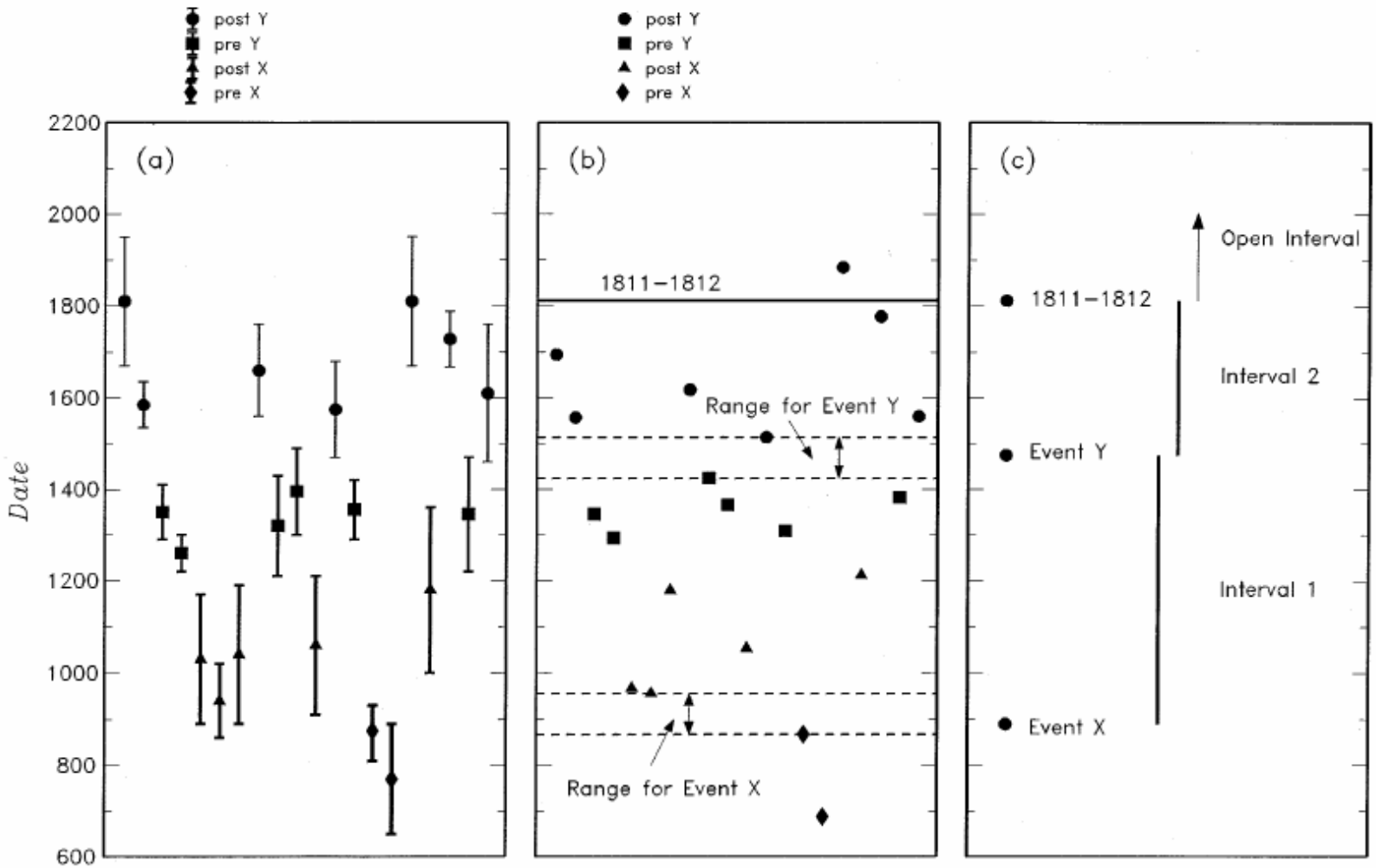

Seismic Hazards Report for the EGC ESP Site

Illustration of Simulation Process for Evaluating Time Intervals between Characteristic New Madrid Earthquakes

Figure
B-2-1

Non-GDS

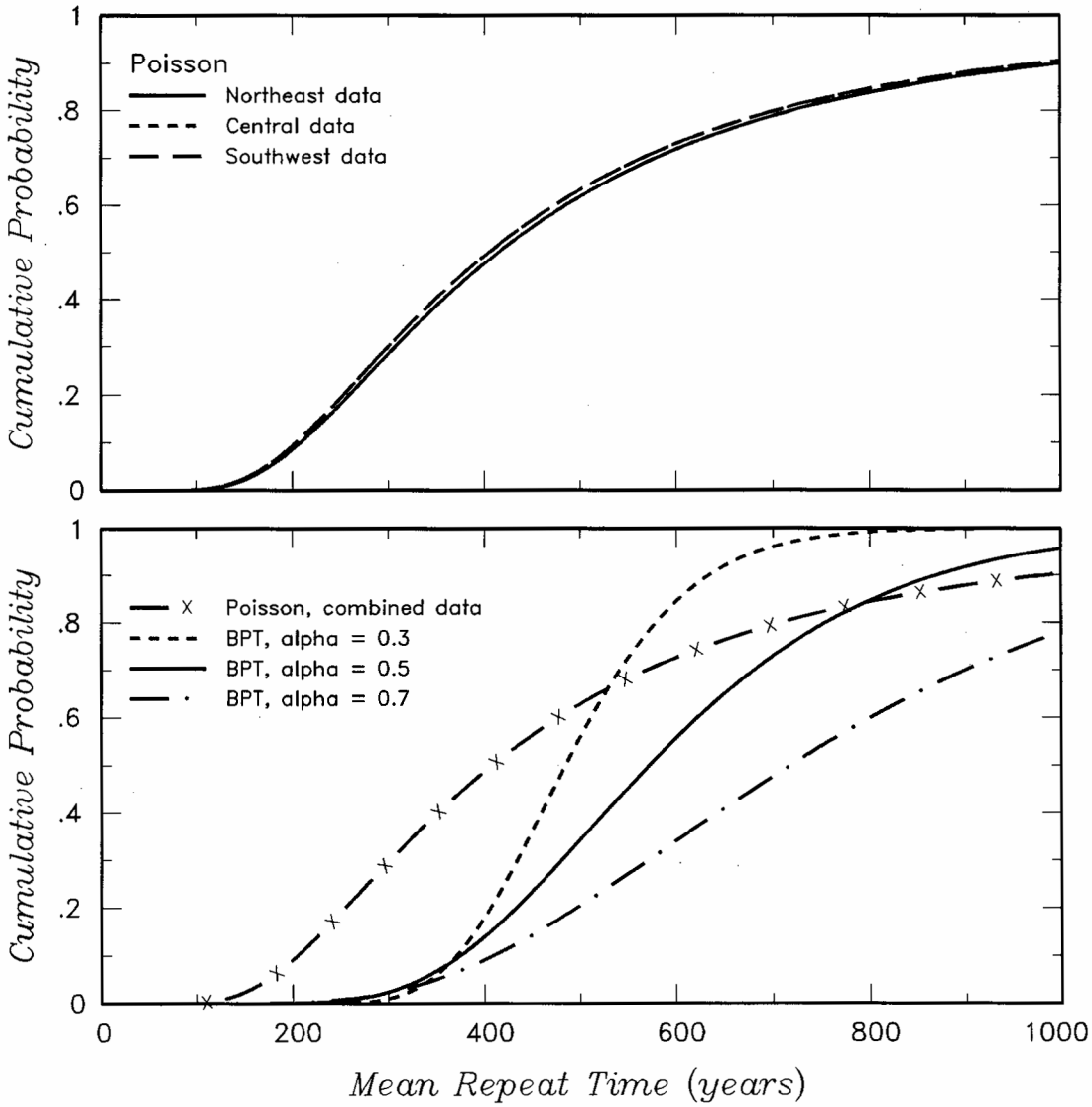

Seismic Hazards Report for the EGC ESP Site

Mean Repeat Time for New Madrid Characteristic Earthquakes

Figure
B-2-2